A gene encoding maize caffeoyl-CoA *O*-methyltransferase confers quantitative resistance to multiple pathogens

Qin Yang[1], Yijian He[1], Mercy Kabahuma[2], Timothy Chaya[3], Amy Kelly[1], Eli Borrego[4], Yang Bian[5], Farid El Kasmi[6], Li Yang[6], Paulo Teixeira[6], Judith Kolkman[7], Rebecca Nelson[7], Michael Kolomiets[4], Jeffery L Dangl[6], Randall Wisser[3], Jeffrey Caplan[3,8], Xu Li[9], Nick Lauter[2,10] & Peter Balint-Kurti[1,11]

Alleles that confer multiple disease resistance (MDR) are valuable in crop improvement, although the molecular mechanisms underlying their functions remain largely unknown. A quantitative trait locus, *qMdr*$_{9.02}$, associated with resistance to three important foliar maize diseases—southern leaf blight, gray leaf spot and northern leaf blight—has been identified on maize chromosome 9. Through fine-mapping, association analysis, expression analysis, insertional mutagenesis and transgenic validation, we demonstrate that *ZmCCoAOMT2*, which encodes a caffeoyl-CoA *O*-methyltransferase associated with the phenylpropanoid pathway and lignin production, is the gene within *qMdr*$_{9.02}$ conferring quantitative resistance to both southern leaf blight and gray leaf spot. We suggest that resistance might be caused by allelic variation at the level of both gene expression and amino acid sequence, thus resulting in differences in levels of lignin and other metabolites of the phenylpropanoid pathway and regulation of programmed cell death.

Selection and deployment of crops with MDR conferred by a single locus is a major objective for breeding[1]. Although MDR has been successfully used in crops such as wheat, maize, rice and beans, the molecular mechanisms controlling MDR are largely unknown[1–5]. Several genes providing MDR have been identified from major grass crops, including the wheat genes *Lr67* and *Lr34*, both of which confer quantitative resistance to multiple rust diseases and to powdery mildew and encode a predicted hexose transporter and a putative ABC transporter, respectively[6,7]. *GH3-2*, which encodes an indole-3-acetic acid-amido synthetase[8], has been associated with variation in quantitative resistance to bacterial blight, bacterial streak and blast in rice. No genes underlying MDR in maize have been definitively identified, although a receptor-like kinase, *pan1*, has been implicated as a quantitative susceptibility gene for northern leaf blight (NLB) and Stewart's wilt[9], and association mapping has implicated a glutathione *S*-transferase gene with resistance to southern leaf blight (SLB), NLB and gray leaf spot (GLS)[10].

Plants possess several mechanisms to defend themselves against pathogens. Qualitative or complete resistance is often based on major resistance genes encoding cytoplasmic proteins carrying nucleotide-binding and leucine-rich-repeat domains (NLR proteins). These NLR proteins directly or indirectly detect the presence of pathogen-derived molecules, called effectors, which are introduced into the host cell and facilitate infection[11]. An NLR-protein-mediated defense response is activated after effector recognition and often includes a hypersensitive response (HR; rapid, localized programmed cell death at the point of pathogen penetration) as well as other responses, including ion flux, an oxidative burst, lipid peroxidation and cell-wall fortification[12].

Another widely studied form of resistance known as quantitative disease resistance typically confers partial resistance and is dependent on the segregation of alleles at multiple loci, each with a moderate effect. Numerous studies identifying disease-resistance quantitative trait loci (QTL) have been published[2,13]. In recent years, several genes associated with disease-resistance QTL have been identified[14,15]. These genes all have relatively large effects on disease resistance, as compared with the typically small effects associated with most disease-resistance QTL whose causal variants remain unknown. Mechanisms underlying quantitative resistance are thought to be more diverse than those responsible for qualitative resistance. In some cases, weak NLR-mediated resistance may confer quantitative resistance[16].

Fungal diseases are a major constraint to the production of maize (*Zea mays*. L), one of the world's most widely used crops[17]. Quantitative resistance is used more frequently in maize than in

[1]Department of Entomology and Plant Pathology, North Carolina State University, Raleigh, North Carolina, USA. [2]Department of Plant Pathology and Microbiology, Iowa State University, Ames, Iowa, USA. [3]Department of Plant and Soil Sciences, University of Delaware, Newark, Delaware, USA. [4]Department of Plant Pathology and Microbiology, Texas A&M University, College Station, Texas, USA. [5]Department of Crop Science, North Carolina State University, Raleigh, North Carolina, USA. [6]Howard Hughes Medical Institute, Department of Biology, University of North Carolina at Chapel Hill, Chapel Hill, North Carolina, USA. [7]School of Integrative Plant Science, Cornell University, Ithaca, New York, USA. [8]Department of Biological Sciences, University of Delaware, Newark, Delaware, USA. [9]Plants for Human Health Institute, Department of Plant and Microbial Biology, North Carolina State University, Kannapolis, North Carolina, USA. [10]USDA-ARS Corn Insects and Crop Genetics Research Unit, Ames, Iowa, USA. [11]USDA-ARS Plant Science Research Unit, Raleigh, North Carolina, USA. Correspondence should be addressed to P.B.-K. (peter.balint-kurti@ars.usda.gov) or Q.Y. (qyang6@ncsu.edu).

Received 31 January; accepted 23 June; published online 24 July 2017; doi:10.1038/ng.3919

other major grass crops, such as wheat and rice, which rely more on qualitative resistance to protect yield[13]. To date, seven maize resistance genes have been definitively identified. These include the two qualitative genes *hm1* (encoding a NADPH-dependent HC-toxin reductase conferring resistance against *Cochliobolus carbonum* race 1) and *Rp1-D* (an NLR allele conferring resistance to common rust) and the five major-effect quantitative genes *Rcg1* (an NLR gene conferring resistance to anthracnose stalk rot), *Rxo1* (a maize NLR gene conferring resistance to bacterial streak disease in rice), *ZmWAK* (a wall-associated receptor–like kinase gene underlying a major QTL conferring resistance to head smut), *Htn1* (a wall-associated receptor–like kinase gene conferring quantitative resistance to NLB) and *ZmTrxh* (an atypical thioredoxin gene conferring resistance to sugarcane mosaic virus in maize)[18–24].

SLB (causal agent *Cochliobolus heterostrophus*), GLS (causal agent *Cercospora zeae-maydis*) and NLB (causal agent *Setosphaeria turcica*) are all widespread and economically damaging foliar fungal diseases of maize[10]. All are predominantly necrotrophic, although NLB has been described as hemibiotrophic[22]. Resistance to these diseases is primarily controlled by multiple disease-resistance small-effect QTL[25–27], although several major-effect QTL for NLB have been characterized[22]. Strong genetic correlations for resistance to the three diseases have been reported in different populations[3,10]. We have shown that a QTL on maize chromosome 9, in bin 9.02 (ref. 28), which we have previously called 9B, and which we refer to here as $qMdr_{9.02}$, is associated with resistance to SLB, NLB and GLS[29]. The allele conferring resistance to all these diseases is derived from the maize line NC250 and the susceptibility allele from the commonly used maize line B73. In a separate study, a QTL associated with GLS resistance has been identified at the same region in bin 9.02 in a teosinte introgression population[30]. Genome-wide association studies in the maize nested association mapping (NAM) population composed of 5,000 recombinant inbred lines derived from 26 diverse parents[31] has identified variants in this region significantly associated with resistance to both SLB and GLS[25,32]. Here, using fine-mapping and analysis of insertional mutants and overexpression lines, we identified a caffeoyl-CoA *O*-methyltransferase (CCoAOMT) gene, *ZmCCoAOMT2*, as the gene underlying the resistance effect at $qMdr_{9.02}$. We provide evidence of the resistance mechanism and show that a *ZmCCoAOMT2* homolog is also associated with MDR in *Arabidopsis*.

RESULTS

High-resolution mapping of $qMdr_{9.02}$

We created a near-isogenic line (NIL) called $B73Mdr_{9.02}$ by repeated backcrossing of NC292 to B73 with marker-assisted selection. Analysis of 56,110 markers showed that the NILs were 97.9% genetically similar, and the only identified introgression differentiating the NILs was at bin 9.02 (**Fig. 1a**). As expected, $B73Mdr_{9.02}$ was slightly more resistant to SLB and GLS than its susceptible recurrent parent B73 in the field (**Fig. 1b**,**c** and **Supplementary Fig. 1**). To fine-map $qMdr_{9.02}$, we generated an F_2 population of 972 plants from a cross between B73 and $B73Mdr_{9.02}$ and screened them for recombination events between the two SNPs PZA02344 and PZA03416, which flank $qMdr_{9.02}$ (refs. 27,30,32,33). Subsequently, 636 F_3 plants and 309 F_4 plants from this population were also screened for recombination events in $qMdr_{9.02}$. 54 recombination events were identified, and lines homozygous for each event were generated, genotyped with a set of molecular markers in the $qMdr_{9.02}$ region and evaluated for resistance to SLB and GLS in replicated field trials. Each of the recombinant progeny showed the same resistance pattern to SLB and GLS (**Fig. 1d** and **Supplementary Table 1**). This result resolved $qMdr_{9.02}$ as a QTL for resistance to SLB and GLS within a ~100-kb interval flanked by the SNP markers M1626 and M1636 (**Fig. 1d** and **Supplementary Table 2**).

ZmCCoAOMT2 is the gene underlying the resistance effect at $qMdr_{9.02}$

We performed association analysis as follows. The $qMdr_{9.02}$ region contains four predicted protein-coding genes, on the basis of the B73 reference genome[34], including *GRMZM2G481291* (denoted *ZmFBXL* herein), which encodes an F-box domain and a leucine-rich-repeat domain protein; *ZmCCoAOMT2* (also known as *GRMZM2G099363*), which encodes a caffeoyl-CoA *O*-methyltransferase; GRMZM2G099324 (denoted *ZmRLK* herein), which encodes an S-locus receptor-like protein kinase; and GRMZM2G440198 (denoted *ZmPIF* herein), which encodes a PIF/Ping-Pong family plant transposase (**Fig. 1e** and **Supplementary Table 3**). No additional genes were identified in this region in the genomic sequences of the maize inbred lines F7 (ref. 35), EP1 (ref. 35), CML247 (ref. 36), PH207 (ref. 37), B104 (available in the MaizeGDB database; URLs) or W22 (available at the UCSC Genome Browser for maize; URLs). Because three of the four genes, *ZmFBXL*, *ZmCCoAOMT2* and *ZmRLK*, are homologous to genes with probable roles in plant defense[38,39], we considered them as the most promising candidates. We determined and compared the nucleotide sequences of the coding regions of the three genes in B73 and $B73Mdr_{9.02}$. Small variations were found among the alleles for all three genes (**Supplementary Figs. 2** and **3**).

We performed a $qMdr_{9.02}$ region-specific association analysis by imputing the parental genotypes onto the NAM population that has previously been evaluated for SLB resistance[25,32]. Using 444 molecular markers for the 26 NAM parental lines[40] in the 100-kb $qMdr_{9.02}$ region, of which 38 were from resequencing of *ZmCCoAOMT2*, and the rest were from maize HapMap3 (**Supplementary Table 4** and **Supplementary Fig. 4**), we observed relatively low levels of founder linkage disequilibrium (**Fig. 2a**). The most significant variant ($P = 2.9 \times 10^{-15}$) was located within the 3′ untranslated region (3′ UTR) of *ZmCCoAOMT2* (**Fig. 2a** and **Supplementary Table 5**), a result consistent with our previous analysis using fewer markers[32].

We then performed expression analyses of all three genes in juvenile leaves, comparing the NILs under *C. heterostrophus*–inoculated and noninoculated (mock) conditions. All three genes were expressed in both resistant and susceptible NILs. *ZmFBXL* and *ZmRLK* transcript levels showed no increase after inoculation, nor were any substantial differences observed between the NILs. Only *ZmCCoAOMT2* was induced by infection (**Fig. 2b**–**d**). Furthermore, it was induced more rapidly in $B73Mdr_{9.02}$ than in B73. At both 6 and 12 h postinoculation (hpi), levels of *ZmCCoAOMT2* transcript were substantially higher in $B73Mdr_{9.02}$ than in B73, but at 48 hpi, the transcript levels were similar. The expression and association mapping studies strongly suggested that *ZmCCoAOMT2* was the causal gene for *qMdr9.02*, and subsequent studies were performed to test this hypothesis.

We performed transgenic overexpression as follows. We obtained full-length cDNA for *ZmCCoAOMT2* from B73, $B73Mdr_{9.02}$ and CML333, the NAM parental allele with the largest effect at this QTL[32]. The predicted proteins were 267, 264 and 261 amino acids in B73, $B73Mdr_{9.02}$ and CML333, respectively. Sequence analysis revealed a deletion of three amino acids in the first exon in $B73Mdr_{9.02}$, and a deletion of two amino acids at the same position in CML333 compared with B73. Additionally, we observed two separate amino acid substitutions in the third exon in $B73Mdr_{9.02}$ compared with B73, and four amino acids deleted at the end of the first exon in CML333 compared with B73 and $B73Mdr_{9.02}$. (**Supplementary Figs. 2**–**4**). We transformed the susceptible maize inbred line B104 with an expression cassette in

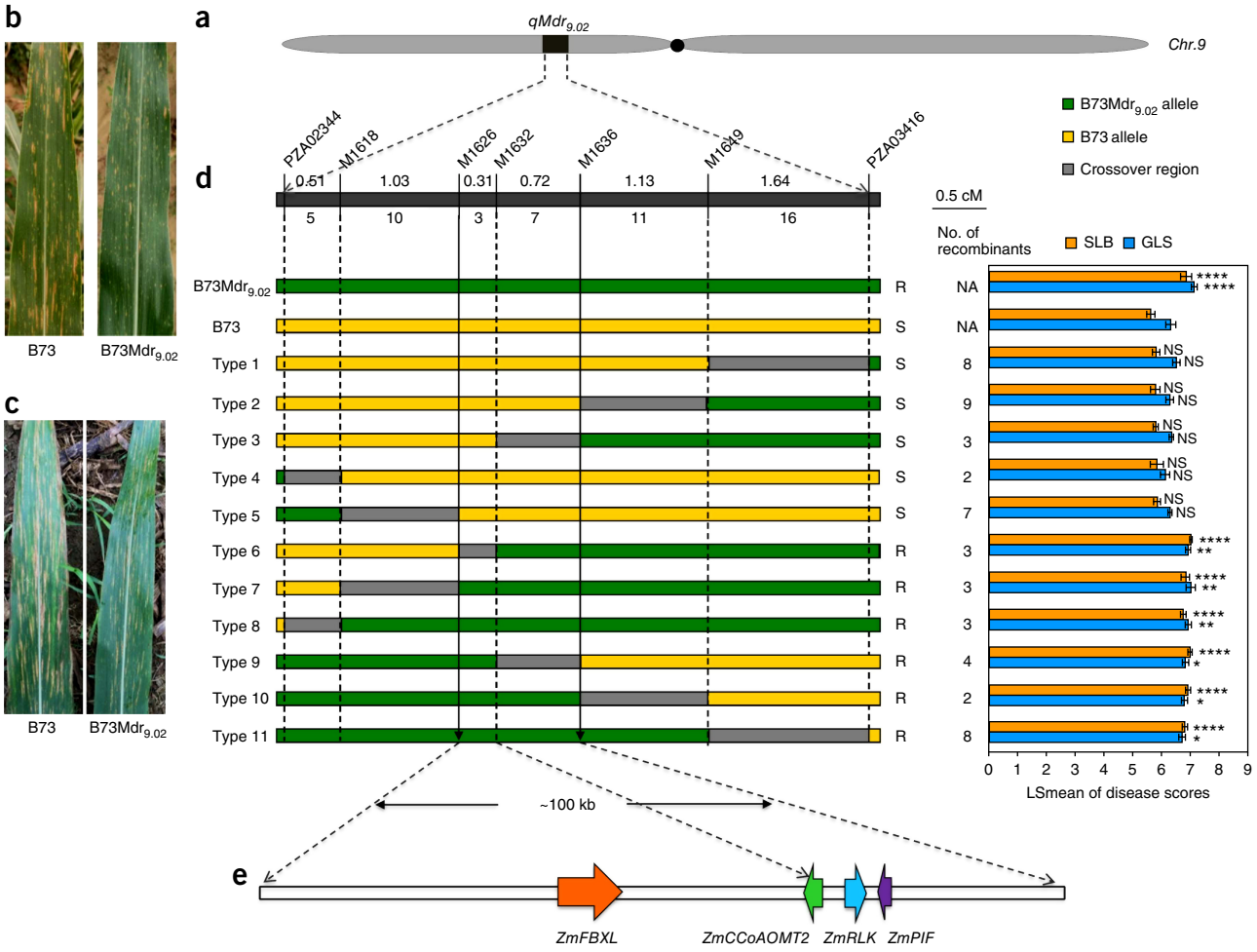

Figure 1 Phenotype and fine-mapping of *qMdr*$_{9.02}$. (**a**) Chromosome location of the *qMdr*$_{9.02}$ region in bin 9.02. (**b**,**c**) Ear leaves of typical B73 and B73Mdr$_{9.02}$ plants infected with SLB (**b**) and GLS (**c**). Pictures were taken of neighboring plants on the same day. B73Mdr$_{9.02}$ showed increased resistance to both SLB and GLS. (**d**) High-resolution mapping delimited *qMdr*$_{9.02}$ to a ~100-kb physical interval flanked by markers M1626 and M1636 for both SLB and GLS resistance. The parental lines B73Mdr$_{9.02}$ and B73 are shown at the top, and the homozygous recombinants are in 11 groups defined by marker genotype. Recombination breakpoints for important recombinants are shown in gray. Green segments represent the B73Mdr$_{9.02}$ allele, and yellow segments represent the B73 allele. Only critical markers representing recombination breakpoints are indicated. The number of recombinants is shown below the markers. Relative genetic distance is shown between markers. The number of recombinants in each recombination type is indicated. NA, not applicable; R, resistant; S, susceptible. The disease resistance was rated with a nine-point scale, with 1 being dead and 9 being the most resistant. Least-square means (LSmeans) of SLB and GLS of homozygous progeny of each recombinant are shown in the bar chart. Error bars, s.e. of the LSmeans. Tukey's test (two tailed) indicates a significant difference between each recombination type and B73. ****$P < 0.0001$; **$P < 0.01$; *$P < 0.05$; NS, not significant. Detailed statistics are shown in **Supplementary Table 1**. (**e**) The *qMdr*$_{9.02}$ region contains four predicted genes.

which expression of the *ZmCCoAOMT2* allele from the maize line CML333 was driven by the maize ubiquitin promoter (**Fig. 3a**).

To evaluate SLB resistance, we performed replicated field trials on T_1 families derived by self-pollination of five independent T_0 transformants. Expression of *ZmCCoAOMT2* was measured in at least five transgenic and three nontransgenic plants chosen at random from each family. In three of five T_1 families, the transgenic lines showed significantly increased SLB resistance compared with that of their nontransgenic siblings (**Fig. 3b** and **Supplementary Table 6**). Transgenic plants from these three populations (events A693B2, A693B5 and A693B8) had median levels of *ZmCCoAOMT2* transcript accumulation 8- to16-fold higher than that of B104, whereas the median *ZmCCoAOMT2* transcript accumulation was 2.5 fold higher in the other two families (events A693B3 and A693B7; **Fig. 3c**). We plotted the relationship between SLB resistance and *ZmCCoAOMT2* transcript accumulation for the 46 T_1 individual plants for which we had both of these data points, and we found that these traits were highly correlated (**Supplementary Fig. 5**; $P < 0.0001$). We inoculated T_2-backcrossed transgenic juvenile plants from event A693B5 with *C. heterostrophus* in a growth chamber. The transgenic-positive plants had significantly less necrosis on the infected leaf than did their nontransgenic siblings (**Supplementary Fig. 6**).

We performed analysis of transposon-insertion lines as follows. The maize UniformMu resource is a collection of lines carrying sequence-indexed insertions of the *Mutator* (*Mu*) transposon throughout the genome in the background of the maize inbred line W22 (ref. 41). We identified two maize insertion lines, Mu270 and Mu619, which carried the same *Mu* insertion (mu1005988) in the 3′-UTR region of *ZmCCoAOMT2* (**Fig. 4a**). Mu270 and Mu619 plants homozygous for this insertion showed significantly increased resistance to both SLB and GLS compared with that of W22 in replicated field trials (**Supplementary Fig. 7**). Although only one *Mu*-insertion allele has been identified in

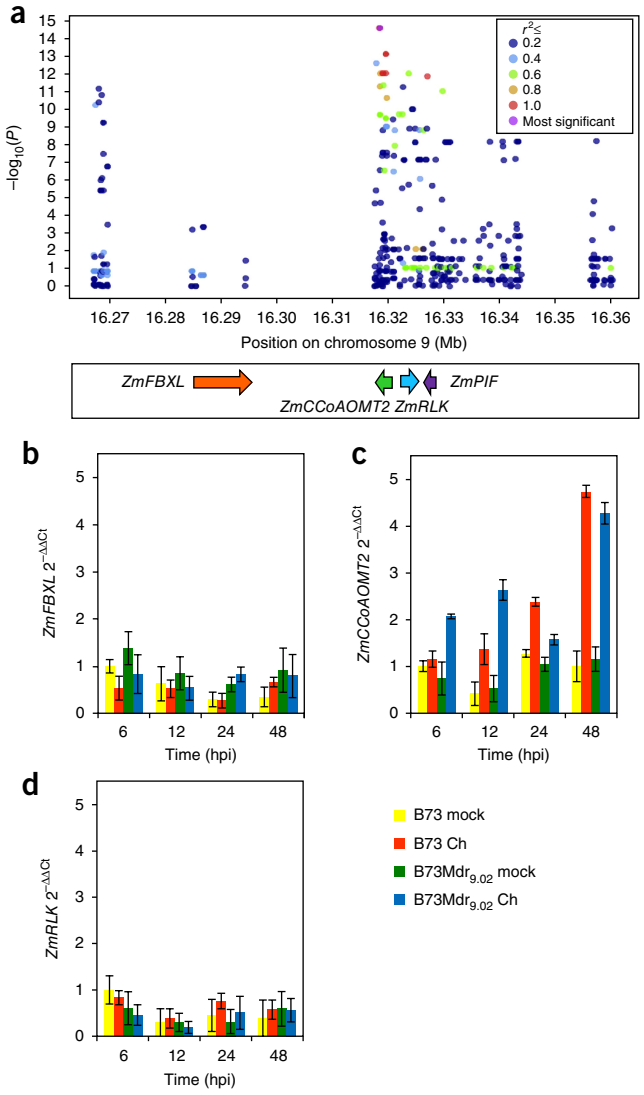

Figure 2 Association and expression analyses of candidate genes in the $qMdr_{9.02}$ region. (**a**) Distribution of $-\log_{10}(P)$ of variants associated with SLB resistance in the $qMdr_{9.02}$ region in the NAM population. Detailed statistics are shown in Online Methods. Chromosomal physical position (AGP_V2) is indicated on the *x* axis. The most significant variant is shown in purple; otherwise, the colors represent their linkage disequilibrium (r^2) with the most significant variant. Positions of predicted genes within the $qMdr_{9.02}$ region are shown at the bottom. (**b**–**d**) Dynamic candidate-gene expression profiles in NILs after *C. heterostrophus* infection in juvenile leaves. Relative expression of *ZmFBXL* (**b**), *ZmCCoAOMT2* (**c**) and *ZmRLK* (**d**) after inoculation on the fifth leaves at 6, 12, 24 and 48 h postinoculation (hpi) are shown. The expression values presented are relative to those in B73 at 6 h after mock infection. B73 Ch and $B73Mdr_{9.02}$ Ch represent pathogen-infected samples, and B73 mock and $B73Mdr_{9.02}$ mock indicates mock-infected samples. Bars indicate s.e. of three technical replicates. The experiment was repeated independently three times and yielded comparable results.

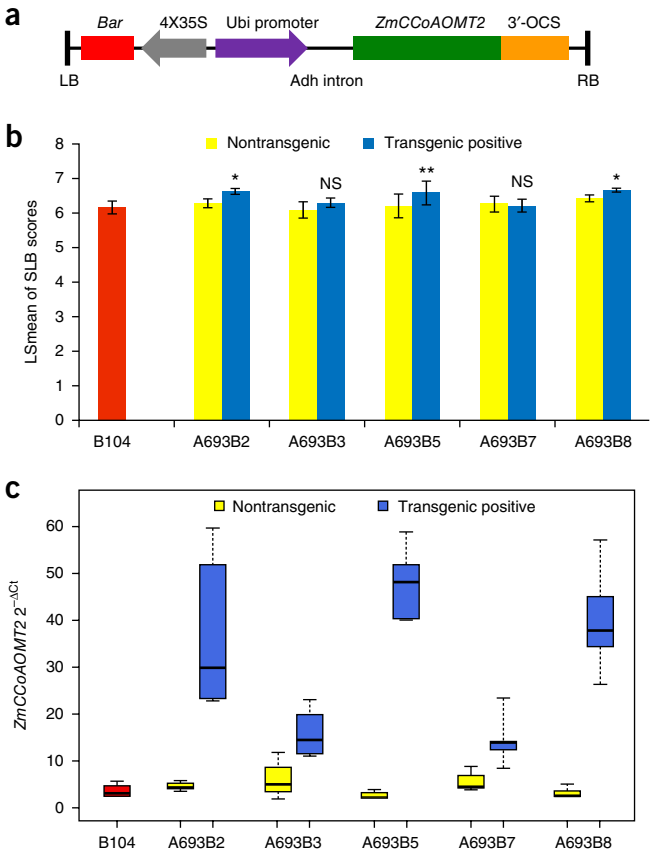

Figure 3 Transgenic overexpression of *ZmCCoAOMT2*. (**a**) Structure of the overexpression construct of *ZmCCoAOMT2* used in the maize transformation experiments. Expression of *ZmCCoAOMT2* was driven by the maize ubiquitin promoter. LB, left border; RB, right border; Ubi promoter, ubiquitin promoter; OCS, octopine synthase gene; Bar, Basta-resistance gene. (**b**) SLB-resistance performance of transgenic plants in the field. Five transgenic events A693B2, A693B3, A693B5, A693B7 and A693B8, as well as the transgenic receptor line B104 were included. The disease resistance was rated with a nine-point scale, with 1 being dead and 9 being the most resistant. Error bars, s.e. of the LSmeans. Tukey's test (two tailed) indicated a significant difference between nontransgenic and transgenic-positive plants in each family. $^{**}P < 0.01$; $^{*}P < 0.05$; NS, not significant. Detailed statistics are shown in **Supplementary Table 6**. (**c**) The relative expression levels of *ZmCCoAOMT2* in the transgenic lines for each of the five events. The expression level of each genotype in each event was an average of expression from 3 individual plants for nontransgenic genotype and 5 individual plants for transgenic-positive genotype. Gene expression was measured relative to the housekeeping gene *ZmTubulin4*. In each box-and-whisker plot, the center line is the median. The bottom and top edges of the boxes indicate the twenty-fifth and seventy-fifth percentiles. Whiskers mark the range of the data, excluding outliers.

these two UniformMu lines, we could not rule out the possibility that other insertions or genomic modifications might exist that differentiate them from W22, and that the increased resistance observed might have been caused by one of these unidentified modifications. To address this possibility, we generated four populations of $F_{2:3}$-segregating families from crosses between each of the insertion lines and W22 in both directions and tested them for resistance to SLB and GLS in replicated trials. In each of these four populations, $F_{2:3}$ families homozygous for the insertion at *ZmCCoAOMT2* were significantly more resistant to both diseases than $F_{2:3}$ families homozygous for the absence of the insertion (**Fig. 4b**–**c** and **Supplementary Table 7**). We investigated the expression of the three candidate genes in the insertion lines. In agreement with our expectations, only *ZmCCoAOMT2* expression was induced by *C. heterostrophus* infection, and earlier and greater induction occurred in the insertion line than its wild-type counterpart (**Fig. 4d**–**f**).

Arabidopsis CCoAOMT1* may play a similar role in *Arabidopsis

Seven paralogs of the *CCoAOMT* gene family were identified in the *Arabidopsis* genome[42], and six members were identified in the maize

B73 genome. The closest *Arabidopsis* homolog of *ZmCCoAOMT2* is at locus *AT4G34050* (*CCoAOMT1* herein) (**Supplementary Fig. 8**). To determine whether *Arabidopsis CCoAOMT1* is involved in disease resistance, we assessed two *Arabidopsis* mutants with T-DNA insertions in this gene, *ccoaomt1-3* and *ccoaomt1-5* (ref. 43), for disease resistance against the bacterial pathogen *Pseudomonas syringae pv tomato* (*Pto*) DC3000 either with or without the avriulence gene *avrRpt2*, and against the oomycete pathogen *Hyaloperonospora arabidopsidis* (*Hpa*, isolates *Emwa1* and *Noco2*). Both *ccoaomt1-3* and *ccoaomt1-5* mutants, compared with wild type Col-0, showed slightly increased susceptibility to both pathogens (**Supplementary Fig. 9**). Publicly available RNA-seq and microarray data indicate that *Arabidopsis CCoAOMT1* is upregulated after pathogen infection or induction of the defense response (**Supplementary Fig. 10**).

Together, these data support our hypothesis that *ZmCCoAOMT2* is involved in disease resistance to multiple pathogens and that it underlies the effect of $qMdr_{9.02}$, as well as that this resistance is associated with increased gene expression after infection. Our results also suggest that similar mechanisms may function in *Arabidopsis* and in other plant species.

ZmCCoAOMT2 controls metabolite levels in the phenylpropanoid and lipoxygenase pathways

ZmCCoAOMT2 is predicted to be involved in lignin biosynthesis as part of the phenylpropanoid pathway[44]. To investigate the effect of $qMdr_{9.02}$ on secondary metabolites, extracts from B73 and $B73Mdr_{9.02}$ ear leaves infected with SLB and displaying the expected differential resistance were used for untargeted metabolite profiling by liquid chromatography–mass spectrometry (LC–MS). Notably, accumulation of the lignin precursor coniferin was significantly higher in $B73Mdr_{9.02}$ than in B73 (**Fig. 5a**). Similarly, we observed that coniferin accumulated to higher levels in the Mu270 and Mu619 plants homozygous for the *Mu* insertion at *ZmCCoAOMT2* than in W22 (**Fig. 5b**). We identified 14 other metabolites without annotated functions whose levels were significantly different between B73 and $B73Mdr_{9.02}$ or between the insertion lines Mu270 and Mu619 and W22. For each metabolite, the changes were in a consistent direction in each of the two resistant/susceptible NIL comparisons (**Supplementary Fig. 11**).

Multiphoton excitation of lignin autofluorescence has previously been used to map the distribution of lignin[45]. To examine whether $qMdr_{9.02}$ affects lignin content after *C. heterostrophus* infection, we investigated two NILs that differed for the minimal 100-kb region defining $qMdr_{9.02}$ (type 6 NIL-R and type 3 NIL-S; recombinants shown in **Fig. 1d**). 770-nm multiphoton excitation was used to detect lignin autofluorescence in paraffin cross-sections of leaves of the NILs at 6 and 12 hpi with *C. heterostrophus*. Spectral unmixing of the lignin autofluorescence showed lignification in the xylem, bundle sheaths and outer surfaces of the epidermal tissue layers (**Fig. 5c**). We verified this cellular distribution with acriflavine staining[46] (**Fig. 5d**). Quantification of fluorescence showed a significant increase in lignin in the bundle sheaths and xylem of NIL-R 12 hpi compared with the susceptible NIL-S at 6 or 12 hpi (**Fig. 5e–i**).

Metabolites from the lipoxygenase pathway, called oxylipins, have been reported to be involved in plant defense responses either as hormone-like signals or as a result of direct antimicrobial activities[47]. To examine whether $qMdr_{9.02}$ affects oxylipin and phytohormone content after *C. heterostrophus* infection, we investigated NIL-R and NIL-S by using a targeted LC–MS/MS system. NIL-S accumulated higher levels of the phytohormones cinnamic acid and traumatic acid than NIL-R at 24 h after treatment (**Supplementary Fig. 12a,b**). NIL-R accumulated higher levels of several oxylipins than NIL-S in either mock/*C. heterostrophus*-infected plants at 24 hpi or nontreated plants at 0 hpi (**Supplementary Fig. 12 c–i**). Several oxylipin-biosynthesis genes have been shown to have roles in resistance to a number of diseases including SLB[47,48].

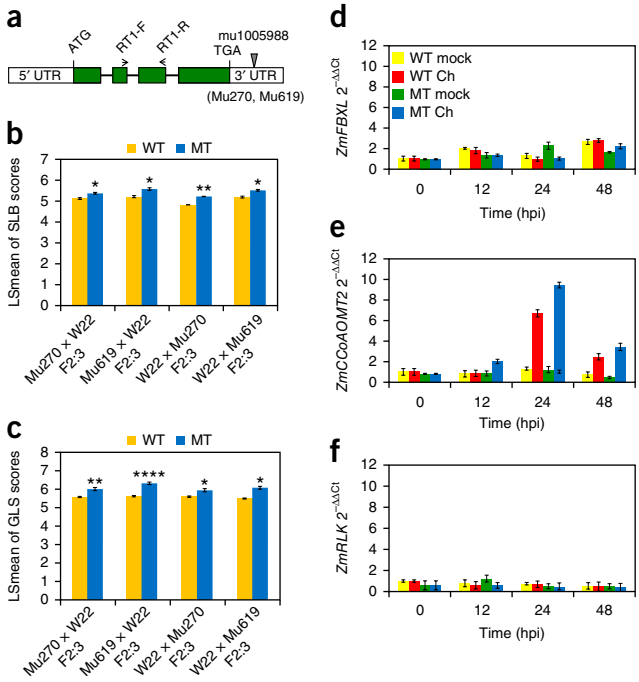

Figure 4 Evaluation of transposon-insertion lines. (**a**) Schematic of *Mutator* insertions relative to *ZmCCoAOMT2* in maize line W22. Protein-coding regions are indicated as green bars. UTRs are indicated as white bars. The *Mutator* insertion is indicated by a gray triangle. Primers (RT1-F and RT1-R) used for quantitative RT–PCR of *ZmCCoAOMT2* are indicated. (**b**,**c**) Disease-resistance performance of four segregating $F_{2:3}$ families of two *Mutator*-insertion lines for SLB (**b**) and GLS (**c**) in the field. The disease resistance was rated with a nine-point scale, with 1 being dead and 9 being the most resistant. Error bars, s.e. of the LSmeans. Tukey's test (two tailed) indicates a significant difference between the insertion line and its wild type in each family. $^{****}P < 0.000$; $^{**}P < 0.01$; $^{*}P < 0.05$; MT, insertion lines; WT, wild-type lines. Detailed statistics can be found in **Supplementary Table 7**. (**d**–**f**) Dynamic candidate-gene expression profiles in the homozygous insertion line and its wild type generated from Mu619 and W22 after infection with *C. heterostrophus* in juvenile leaves. Relative transcript levels of *ZmFBXL* (**d**), *ZmCCoAOMT2* (**e**) and *ZmRLK* (**f**) at 0, 12, 24 and 48 h post inoculation (hpi) with *C. heterostrophus* are shown. WT Ch and MT Ch represent pathogen-infected samples, and WT mock and MT mock indicate mock-infected samples. The expression values are presented relative to those in wild type at 0 h after mock infection. Bars, s.e. of three technical replicates. The experiment was repeated independently three times and yielded comparable results.

Suppression of programed cell death by *ZmCCoAOMT2* may contribute to disease resistance

ZmCCoAOMT2 has previously been identified as a suppressor of HR induced by the maize autoactive NLR-protein Rp1-D21 (refs. 49,50). HR is often believed to be beneficial to necrotrophic pathogens[51] such as the fungi causing SLB and GLS. We sought to determine whether suppression of HR by *ZmCCoAOMT2* might cause disease resistance. $qMdr_{9.02}$ was identified as a QTL in the NAM population for both SLB resistance and HR suppression, and in each case, effect estimates have been calculated for the alleles from 24 out of 25 non-B73 parents

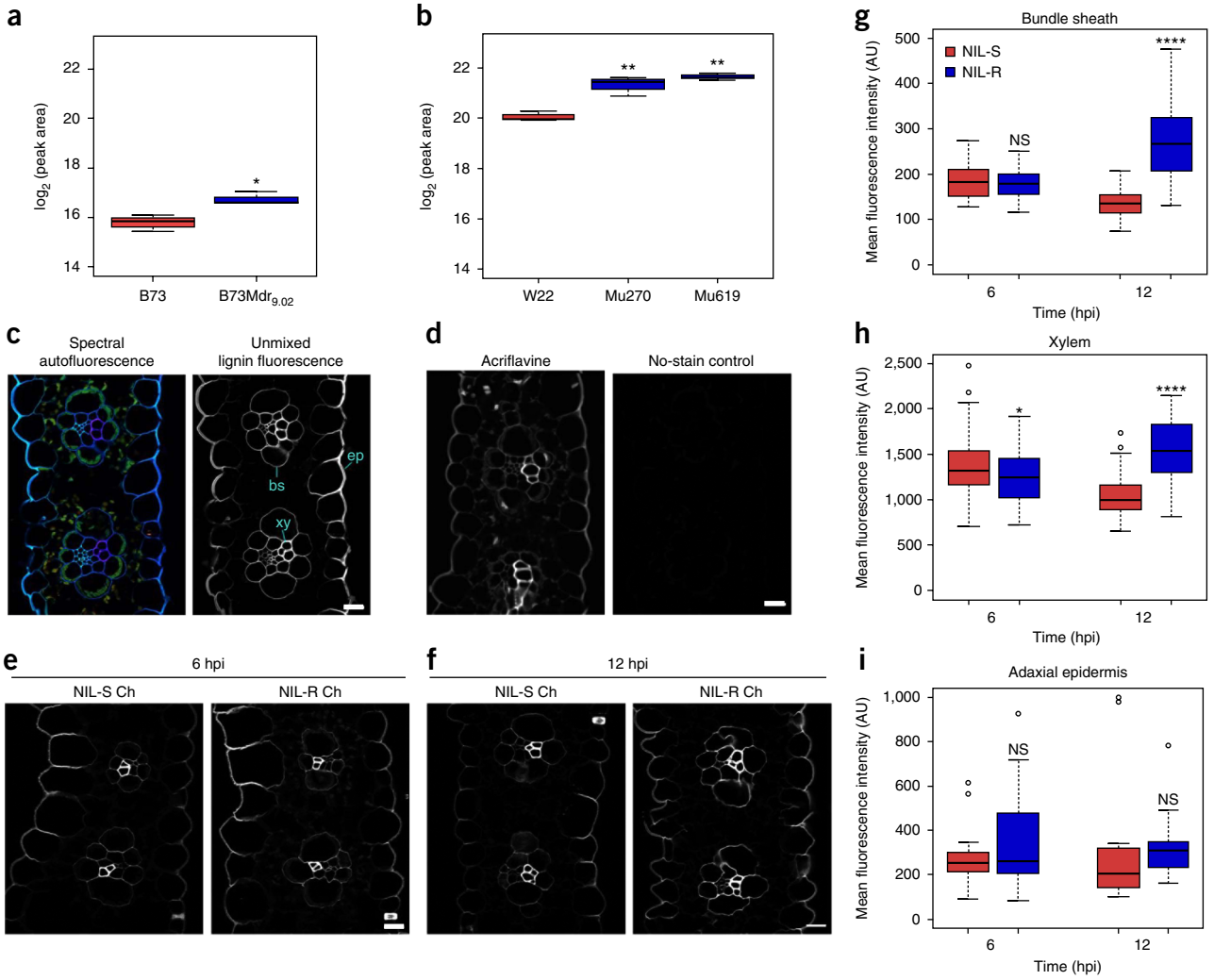

Figure 5 Differential levels of lignin and lignin precursors identified in resistant and susceptible NILs. (**a**,**b**) Relative abundance of coniferin content in ear leaves infected with SLB in the field in the parental lines (**a**) and the *Mutator*-insertion lines (**b**). $^{**}P < 0.01$; $^{*}P < 0.05$ by Student's *t*-test with Welch's correction (two tailed). Sample sizes, $n = 3$ independent experiments. (**c**–**i**) Characterization of lignification. (**c**) Paraffin sections imaged with 770-nm multiphoton excitation to induce lignin autofluorescence. The spectral images show a combination of lignin autofluorescence (blue) and background autofluorescence (green and red). Unmixed lignin autofluorescence shows lignification in the cell walls of the bundle sheath (bs), xylem (xy) and epidermis (ep). (**d**) Verification of the location of lignification with acriflavine staining. A sample without stain was used as a control. (**e**,**f**) Representative images of lignin fluorescence from NILs infected with *C. heterostrophus* and fixed at 6 and 12 h post inoculation (hpi). (**c**–**f**) Scale bars, 20 µm. (**g**–**i**) Quantification of the lignin fluorescence intensity (AU, arbitrary units) in bundle sheath (**g**), xylem (**h**) and adaxial epidermis (**i**). Symbols at top indicate significant differences between NIL-S and NIL-R, as determined by Student's *t*-test with Welch's correction (two tailed). $^{*}P < 0.05$; $^{****}P < 0.0001$; NS, not significant. Sample sizes are $n = 58$ bundle sheaths per group (**g**), $n = 58$ xylems per group (**h**), and $n = 29$ images per group (**i**). In each box-and-whisker plot, the center values are the medians. The bottom and top edges of the boxes indicate the twenty-fifth and seventy-fifth percentiles. Whiskers mark the range of the data, excluding outliers.

relative to the B73 allele[32,49]. The allele effect for SLB resistance was significantly negatively correlated with the effect for Rp1-D21-induced HR suppression (Pearson correlation coefficient = 0.45, $P = 0.026$; **Supplementary Fig. 13**), such that increased SLB resistance was correlated with decreased HR, in agreement with our hypothesis.

To determine whether the B73Mdr$_{9.02}$*ZmCCoAOMT2* allele suppressed HR to a greater extent than the B73 allele, we cloned both alleles and transiently coexpressed each of them with Rp1-D21 in *Nicotiana benthamiana*. Suppressed HR was observed in each case (**Fig. 6a**). To quantify the HR suppression, a 'dynamic HR assay' was performed by infiltrating multiple sites on different leaves and monitoring each site for necrosis every day for 4 d (ref. 52 and **Supplementary Fig. 14**). By these criteria, the B73Mdr$_{9.02}$*ZmCCoAOMT2* allele suppressed Rp1-D21-induced HR ~10% more than did the B73 allele (**Fig. 6b** and **Supplementary Fig. 15a**). To examine whether ZmCCoAOMT2 specifically suppressed Rp1-D21-induced HR or was a general HR suppressor, we coexpressed both *ZmCCoAOMT2* alleles with the autoactive *Arabidopsis R* gene *RPM1* encoding a p.Asp505Val substitution[53]. The same suppression pattern was observed, and the B73Mdr$_{9.02}$*ZmCCoAOMT2* allele suppressed RPM1 p.Asp505Val–induced HR ~10–20% more than did the B73 allele (**Fig. 6c** and **Supplementary Fig. 15b**).

DISCUSSION

Quantitative resistance has been widely used in breeding programs in many crop species to provide durable resistance[13]. Few genes underlying quantitative resistance have been cloned, because most

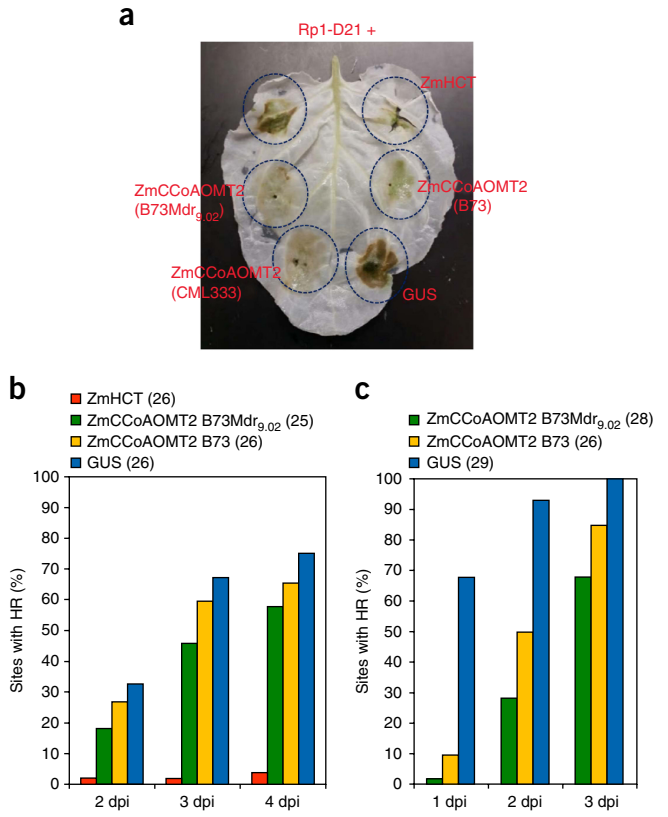

Figure 6 Function of ZmCCoAOMT2 in repressing the hypersensitive response (HR) induced by autoactive NLR proteins. (**a**) *ZmCCoAOMT2* suppresses the HR induced by Rp1-D21 in an *N. benthamiana* leaf. Agroinfiltration sites transiently expressing ZmHCT (suppression control), ZmCCoAOMT2 (alleles from B73, B73Mdr$_{9.02}$ or CML333) or GUS (nonsuppression control) were challenged with *Agrobacterium tumefaciens* expressing Rp1-D21. The photograph was taken at 3 d post infiltration (dpi). (**b**) Percentage of infiltration sites showing HR after coexpression of ZmCCoAOMT2 (from B73Mdr$_{9.02}$ or B73), ZmHCT or GUS with RP1-D21 at 2, 3 and 4 dpi. 25 or 26 infiltration sites were assessed for each gene, as indicated in parentheses. (**c**) Percentage of infiltration sites showing HR after coexpression of ZmCCoAOMT2 (from B73Mdr$_{9.02}$ or B73) or GUS with RPM1 p.Asp505Val at 1, 2 and 3 dpi. 26–29 infiltration sites were assessed for each gene, as indicated in parentheses. The experiments were repeated independently twice and yielded comparable results (**Supplementary Fig. 15**).

disease-resistance QTL have small and somewhat inconsistent effects, thus hindering the reliable association of genotypes with phenotypes. In a previous study using NILs, we have identified a QTL on chromosome 9 that is associated with resistance to SLB, NLB and GLS[29]. In the present study, we fine-mapped this QTL, denoted *qMdr$_{9.02}$*, and identified *ZmCCoAOMT2* as the gene underlying disease resistance to SLB and GLS. Resistance to NLB appeared to be more complex. Our findings (data not shown) suggested that several genes in this region, of which *ZmCCoAOMT2* is one, may underlie NLB resistance. *qMdr$_{9.02}$* has relatively small effects compared with most disease-resistance QTL for which the underlying genes have been identified (**Fig. 1b**,**c**). In the studies in which *qMdr$_{9.02}$* was first identified, this locus accounted for 10% and 6% of the variation for SLB and GLS resistance respectively, in the same biparental mapping population[33,54], and we observed comparable effects in this study. Although the definition of a small-effect QTL is subjective, it is clear that most of the quantitative resistance genes identified to date have caused large effects, and many have been heavily used by breeders as single mendelian loci, just as qualitative disease-resistance genes might be used[6,7,14]. Although these major-effect quantitative resistance genes are important, much of the disease resistance to SLB and GLS that protects plants in the field is based on multiple loci with small effects[25,27].

Positive correlations among resistance to different diseases have been observed in maize in both diverse germplasm populations and biparental families[3,10,17,49]. In most cases, however, the QTL identified in these populations have been disease specific. We have previously hypothesized that the correlations among diseases might be due to QTL with pleiotropic effects on multiple diseases that are too small to be detected individually[1]. This work provides some evidence supporting this hypothesis.

Unlike the other cloned major quantitative resistance genes in maize—*ZmWAK* (ref. 20), *Rcg1* (ref. 21) and *ZmHtn*[22], which have classic resistance-gene structure and probably function in pathogen recognition early in the defense pathway—*ZmCCoAOMT2* appears to function downstream of the recognition event. CCoAOMT has been predicted to be involved in the phenylpropanoid pathway and to be important in lignin biosynthesis. Lignin has long been implicated in plant disease resistance, owing to its function in strengthening the cell wall[55]. Beyond lignin, several other products of the phenylpropanoid pathway, including several phytoalexins, are important in plant defense[56,57]. However, this study is, to our knowledge, the first showing that natural variation underlying one of the genes in this pathway is responsible for quantitative resistance to multiple pathogens.

Differences in expression may be a mechanistic cause of resistance. *ZmCCoAOMT2* expression is induced after pathogen infection in both the resistant and susceptible NILs, and the resistance allele is induced earlier and to higher levels than the susceptibility allele (**Fig. 2c**). Higher expression is also associated with increased resistance in transgenic and UniformMu lines (**Figs. 3c** and **4e** and **Supplementary Fig. 5**). The *Mu* insertion was located in the 3′ UTR of *ZmCCoAOMT2* (**Fig. 4a**), and the most significant variant associated with SLB resistance in NAM population was also in the 3′-UTR region (**Fig. 2a**). Increased accumulation of *ZmCCoAOMT2* mRNA might be associated with 3′-UTR variation, which may regulate mRNA stability after pathogen infection[58]. In *Arabidopsis* Col-0, *Arabidopsis CCoAOMT1* is also induced after pathogen or elicitor treatment (**Supplementary Fig. 10**), thus suggesting that upregulation of *Arabidopsis CCoAOMT1* may be important for its resistance function. The small increase in resistance in the transgenic lines was not proportional to the large increase in gene expression. Metabolic pathways are complex, and the flux through them might not increase proportionally to the increased expression of any specific gene[59].

In agreement with the prediction that ZmCCoAOMT2 functions in the lignin-biosynthesis pathway, we observed increased accumulation of the lignin precursor coniferin and of lignin itself in resistant compared with susceptible NILs differing in their *ZmCCoAOMT2* alleles (**Fig. 5**). Coniferin has previously been implicated in disease resistance in *Arabidopsis*[60]. Levels of cinnamic acid, a product of the first enzyme of the phenylpropanoid pathway, was significantly increased in NIL-S compared with NIL-R at 24 hpi after mock/*C. heterostrophus* treatment (**Supplementary Fig. 12a**). This result might have been due to altered flux through the pathway[61]. These data support roles of ZmCCoAOMT2 in the phenylpropanoid pathway and in lignin production and suggest that resistance may be mediated through increased production of lignin and coniferin in lines carrying the resistance allele at *qMdr$_{9.02}$*. NIL-R and NIL-S also showed differences in the levels of some plant secondary metabolites involved in lipoxygenase pathways (**Supplementary Fig. 12**). Some of these differences may also contribute to disease resistance[62].

We found some evidence that coding variation may also affect resistance. The resistance *ZmCCoAOMT2* allele from B73Mdr$_{9.02}$ suppressed HR induced by both Rp1-D21 and RPM1 p.Asp505Val ~7–21% more than the susceptibility allele from B73, particularly at 2 and 3 d after infiltration (**Fig. 6** and **Supplementary Fig. 15**). This effect may be increased in maize, owing to the higher expression of the resistance allele during infection. We also observed a significant negative correlation between HR and SLB resistance at this QTL in the NAM population (**Supplementary Fig. 13**). This result suggested that ZmCCoAOMT2 is a general suppressor of HR, a process that generally confers resistance to diseases caused by biotrophic pathogens while facilitating the growth of necrotrophic pathogens[51,63]. Thus, more effective suppression of HR, and perhaps other forms of programmed cell death, might lead to increased resistance to necrotrophic diseases such as those causing SLB and GLS. Previously, we have suggested that ZmCCoAOMT2 specifically suppresses HR caused by Rp1-D21 (ref. 50). Here, we used a more sensitive 'dynamic' assay to show that ZmCCoAOMT2 also suppresses HR caused by RPM1 p.Asp505Val. The similar patterns of differential metabolite accumulation between mock and inoculated samples shown in **Supplementary Figure 12** also suggested that coding variation between the resistant and susceptible alleles may have been important.

Although we found that *ZmCCoAOMT2* is associated with variation in resistance at *qMdr$_{9.02}$*, we have not formally ruled out roles in resistance for the other three genes at this locus: *ZmPIF*, *ZmFBXL* and *ZmRLK*. It is possible that one or more of these genes may also be associated with resistance, and *ZmRLK* appears to be the most likely candidate, on the basis of its sequence and the significant associations identified in this region. Furthermore, maize gene content is variable across lines[64]. Notably, in the sequenced maize lines F7, EP1, CML247, PH207, B104 and W22, there are no additional predicted genes in this region, but we did not sequence the corresponding region from NC292, which may possibly contain additional genes with a role in resistance.

In this study, we established the function of *ZmCCoAOMT2* in conferring resistance to SLB and GLS and in underlying the function of the disease-resistance QTL *qMdr$_{9.02}$*. We suggest that resistance might be caused by allelic variation at the levels of both gene expression and amino acid sequence, thus causing differences in the levels of lignin and other metabolites of the phenylpropanoid pathway and regulation of programmed cell death. Although we tested this QTL against only two diseases, it may confer resistance to other diseases, because its probable mechanisms of action are likely to be broadly effective. This hypothesis is supported by the involvement of this gene in disease resistance in *Arabidopsis*. Breeding for durable and multiple disease resistance is a key goal in disease management. Isolation of *ZmCCoAOMT2* should contribute to this objective in maize. Its moderate effects, which would exert low selection pressure, together with its broad-based modes of action would probably make this QTL quite durable.

URLs. MaizeGDB database, http://www.maizegdb.org/; UCSC Genome Browser for maize, http://www.genomaize.org/; Maize Genetics Cooperation Stock Center, http://maizecoop.cropsci.uiuc.edu/; Gramene, http://gramene.org/; Phylogeny.fr platform, http://www.phylogeny.fr/; The Arabidopsis Information Resource (TAIR), https://www.arabidopsis.org/; National Center for Biotechnology Information (NCBI), http://www.ncbi.nlm.nih.gov/.

METHODS

Methods, including statements of data availability and any associated accession codes and references, are available in the online version of the paper.

Note: Any Supplementary Information and Source Data files are available in the online version of the paper.

ACKNOWLEDGMENTS

We thank J. Holland and J. Dunne for help with association analysis and providing the filtered hapmap3 marker set in the *qMdr$_{9.02}$* region in NAM founder lines. We thank W. Boerjan (Ghent University), K. Wang (Iowa State University), D. McCarty (University of Florida), K. Koch (University of Florida) and J. Brumos (North Carolina State University) for providing materials. We thank R. Franks, E. Johannes and S. Sermons for technical assistance. We thank C. Herring, G. Marshall and the staff at Central Crops Research Station for help with field work. We thank C. Saravitz and the staff at the NCSU Phytotron for growth-chamber-trial support. We thank D. Jackson, S. Kamoun, S. Christensen, B. Olukolu and T. Jamann for helpful discussions. We acknowledge the MaizeGDB database (URLs), which was essential to this work. Research was supported by the USDA and United States National Science Foundation grants IOS-1127076 to R.W. and 1444503 to P.B.-K. Purchase of and access to microscopes was made possible by NIH shared instrumentation grant S10 OD016361 and NIH-NIGMS grant P20 GM103446, both to J.C.

AUTHOR CONTRIBUTIONS

Q.Y., initiation of project, experimental design, gene cloning and functional validation, data analyses and writing the manuscript. Y.H., experimental design, HR suppression experiment, bacterial infection assays and writing the manuscript. M.K., generation of transgenic maize lines and seed production. T.C., histological analysis. A.K., participation in genotyping transgenic lines, making Gateway constructs and gene expression analysis. E.B., defense metabolite analysis and discussion. Y.B., candidate region–based association analysis. F.E.K., *Hpa*-isolate Emwa1 infection assays in *Arabidopsis*, expression data analysis and manuscript editing. L.Y., *Hpa*-isolate Noco2 infection assays in *Arabidopsis* and manuscript editing. P.T., *Arabidopsis* gene expression analysis based on published data. J.K. and R.N., generating $F_{2:3}$ families for insertion lines, and conception and planning of the project. M.K., discussion and defense metabolite analysis. J.L.D., *Arabidopsis* pathology assays and manuscript writing and editing. R.W., conception and planning of the project. J.C., conception and planning of the project, and histological analysis. X.L., metabolite profiles and lignin analysis. N.L., conception and planning of the project, and generation of transgenic lines. P.B.-K., initiation of the project, experimental design, conception and planning of the project, and manuscript writing and editing.

COMPETING FINANCIAL INTERESTS

The authors declare no competing financial interests.

1. Wiesner-Hanks, T. & Nelson, R. Multiple disease resistance in plants. *Annu. Rev. Phytopathol.* **54**, 229–252 (2016).
2. Miedaner, T. & Korzun, V. Marker-assisted selection for disease resistance in wheat and barley breeding. *Phytopathology* **102**, 560–566 (2012).
3. Zwonitzer, J.C. *et al.* Mapping resistance quantitative trait loci for three foliar diseases in a maize recombinant inbred line population-evidence for multiple disease resistance? *Phytopathology* **100**, 72–79 (2010).
4. Teran, H., Jara, C., Mahuku, G., Beebe, S. & Singh, S.P. Simultaneous selection for resistance to five bacterial, fungal, and viral diseases in three Andean x Middle American inter-gene pool common bean populations. *Euphytica* **189**, 283–292 (2013).
5. Wisser, R.J., Sun, Q., Hulbert, S.H., Kresovich, S. & Nelson, R.J. Identification and characterization of regions of the rice genome associated with broad-spectrum, quantitative disease resistance. *Genetics* **169**, 2277–2293 (2005).
6. Krattinger, S.G. *et al.* A putative ABC transporter confers durable resistance to multiple fungal pathogens in wheat. *Science* **323**, 1360–1363 (2009).
7. Moore, J.W. *et al.* A recently evolved hexose transporter variant confers resistance to multiple pathogens in wheat. *Nat. Genet.* **47**, 1494–1498 (2015).
8. Fu, J. *et al.* Manipulating broad-spectrum disease resistance by suppressing pathogen-induced auxin accumulation in rice. *Plant Physiol.* **155**, 589–602 (2011).
9. Jamann, T.M., Poland, J.A., Kolkman, J.M., Smith, L.G. & Nelson, R.J. Unraveling genomic complexity at a quantitative disease resistance locus in maize. *Genetics* **198**, 333–344 (2014).
10. Wisser, R.J. *et al.* Multivariate analysis of maize disease resistances suggests a pleiotropic genetic basis and implicates a *GST* gene. *Proc. Natl. Acad. Sci. USA* **108**, 7339–7344 (2011).
11. Bent, A.F. & Mackey, D. Elicitors, effectors, and *R* genes: the new paradigm and a lifetime supply of questions. *Annu. Rev. Phytopathol.* **45**, 399–436 (2007).
12. Coll, N.S., Epple, P. & Dangl, J.L. Programmed cell death in the plant immune system. *Cell Death Differ.* **18**, 1247–1256 (2011).
13. Wisser, R.J., Balint-Kurti, P.J. & Nelson, R.J. The genetic architecture of disease resistance in maize: a synthesis of published studies. *Phytopathology* **96**, 120–129 (2006).

14. Fu, D. *et al.* A kinase-START gene confers temperature-dependent resistance to wheat stripe rust. *Science* **323**, 1357–1360 (2009).
15. Fukuoka, S. *et al.* Loss of function of a proline-containing protein confers durable disease resistance in rice. *Science* **325**, 998–1001 (2009).
16. Yang, Q., Balint-Kurti, P. & Xu, M. Quantitative disease resistance: dissection and adoption in maize. *Mol. Plant* **10**, 402–413 (2017).
17. Pataky, J.K. & Williams, M. Reactions of sweet corn hybrids to prevalent diseases and herbicides. *Midwest Vegetable Variety Trial Rep.* 115–148 (2011).
18. Johal, G.S. & Briggs, S.P. Reductase activity encoded by the *HM1* disease resistance gene in maize. *Science* **258**, 985–987 (1992).
19. Collins, N. *et al.* Molecular characterization of the maize *Rp1-D* rust resistance haplotype and its mutants. *Plant Cell* **11**, 1365–1376 (1999).
20. Zuo, W. *et al.* A maize wall-associated kinase confers quantitative resistance to head smut. *Nat. Genet.* **47**, 151–157 (2015).
21. Broglie, K. *et al.* Polynucleotides and methods for making plants resistant to fungal pathogens. US patent 20080016595 A1 (2006).
22. Hurni, S. *et al.* The maize disease resistance gene *Htn1* against northern corn leaf blight encodes a wall-associated receptor-like kinase. *Proc. Natl. Acad. Sci. USA* **112**, 8780–8785 (2015).
23. Zhao, B. *et al.* A maize resistance gene functions against bacterial streak disease in rice. *Proc. Natl. Acad. Sci. USA* **102**, 15383–15388 (2005).
24. Liu, Q. *et al.* An atypical thioredoxin imparts early resistance to *Sugarcane mosaic virus* in maize. *Mol. Plant* **10**, 483–497 (2017).
25. Kump, K.L. *et al.* Genome-wide association study of quantitative resistance to southern leaf blight in the maize nested association mapping population. *Nat. Genet.* **43**, 163–168 (2011).
26. Poland, J.A., Bradbury, P.J., Buckler, E.S. & Nelson, R.J. Genome-wide nested association mapping of quantitative resistance to northern leaf blight in maize. *Proc. Natl. Acad. Sci. USA* **108**, 6893–6898 (2011).
27. Benson, J.M., Poland, J.A., Benson, B.M., Stromberg, E.L. & Nelson, R.J. Resistance to gray leaf spot of maize: genetic architecture and mechanisms elucidated through nested association mapping and near-isogenic line analysis. *PLoS Genet.* **11**, e1005045 (2015).
28. Davis, G.L. *et al.* A maize map standard with sequenced core markers, grass genome reference points and 932 expressed sequence tagged sites (ESTs) in a 1736-locus map. *Genetics* **152**, 1137–1172 (1999).
29. Belcher, A.R. *et al.* Analysis of quantitative disease resistance to southern leaf blight and of multiple disease resistance in maize, using near-isogenic lines. *Theor. Appl. Genet.* **124**, 433–445 (2012).
30. Lennon, J.R., Krakowsky, M., Goodman, M., Flint-Garcia, S. & Balint-Kurti, P.J. Identification of alleles conferring resistance to gray leaf spot in maize derived from its wild progenitor species teosinte. *Crop Sci.* **56**, 209–218 (2016).
31. McMullen, M.D. *et al.* Genetic properties of the maize nested association mapping population. *Science* **325**, 737–740 (2009).
32. Bian, Y., Yang, Q., Balint-Kurti, P.J., Wisser, R.J. & Holland, J.B. Limits on the reproducibility of marker associations with southern leaf blight resistance in the maize nested association mapping population. *BMC Genomics* **15**, 1068 (2014).
33. Zwonitzer, J.C. *et al.* Use of selection with recurrent backcrossing and QTL mapping to identify loci contributing to southern leaf blight resistance in a highly resistant maize line. *Theor. Appl. Genet.* **118**, 911–925 (2009).
34. Schnable, P.S. *et al.* The B73 maize genome: complexity, diversity, and dynamics. *Science* **326**, 1112–1115 (2009).
35. Unterseer, S. *et al.* European Flint reference sequences complement the maize pan-genome. Preprint at http://www.biorxiv.org/content/early/2017/01/27/103747/ (2017).
36. Lu, F. *et al.* High-resolution genetic mapping of maize pan-genome sequence anchors. *Nat. Commun.* **6**, 6914 (2015).
37. Hirsch, C. *et al.* Draft assembly of elite inbred line PH207 provides insights into genomic and transcriptome diversity in maize. *Plant Cell* **28**, 2700–2714 (2016).
38. Xu, G., Ma, H., Nei, M. & Kong, H. Evolution of F-box genes in plants: different modes of sequence divergence and their relationships with functional diversification. *Proc. Natl. Acad. Sci. USA* **106**, 835–840 (2009).
39. Singh, P. & Zimmerli, L. Lectin receptor kinases in plant innate immunity. *Front. Plant Sci.* **4**, 124 (2013).
40. Bukowski, R. *et al.* Construction of the third generation Zea mays haplotype map. Preprint at http://www.biorxiv.org/content/early/2016/09/16/026963/ (2015).
41. Settles, A.M. *et al.* Sequence-indexed mutations in maize using the UniformMu transposon-tagging population. *BMC Genomics* **8**, 116 (2007).
42. Raes, J., Rohde, A., Christensen, J.H., Van de Peer, Y. & Boerjan, W. Genome-wide characterization of the lignification toolbox in *Arabidopsis*. *Plant Physiol.* **133**, 1051–1071 (2003).
43. Vanholme, R. *et al.* A systems biology view of responses to lignin biosynthesis perturbations in *Arabidopsis*. *Plant Cell* **24**, 3506–3529 (2012).
44. Li, L. *et al.* The maize *brown midrib4* (*bm4*) gene encodes a functional folylpolyglutamate synthase. *Plant J.* **81**, 493–504 (2015).
45. Coletta, V.C., Rezende, C.A., da Conceição, F.R., Polikarpov, I. & Guimarães, F.E.G. Mapping the lignin distribution in pretreated sugarcane bagasse by confocal and fluorescence lifetime imaging microscopy. *Biotechnol. Biofuels* **6**, 43 (2013).
46. Rocha, S. *et al.* Lignification of developing maize (*Zea mays* L.) endosperm transfer cells and starchy endosperm cells. *Front. Plant Sci.* **5**, 102 (2014).
47. Gao, X. *et al.* Disruption of a maize 9-lipoxygenase results in increased resistance to fungal pathogens and reduced levels of contamination with mycotoxin fumonisin. *Mol. Plant Microbe Interact.* **20**, 922–933 (2007).
48. Gao, X. *et al.* Maize 9-lipoxygenase *ZmLOX3* controls development, root-specific expression of defense genes, and resistance to root-knot nematodes. *Mol. Plant Microbe Interact.* **21**, 98–109 (2008).
49. Olukolu, B.A. *et al.* A genome-wide association study of the maize hypersensitive defense response identifies genes that cluster in related pathways. *PLoS Genet.* **10**, e1004562 (2014).
50. Wang, G.F. & Balint-Kurti, P.J. Maize homologs of CCoAOMT and HCT, two key enzymes in lignin biosynthesis, form complexes with the NLR Rp1 protein to modulate the defense response. *Plant Physiol.* **171**, 2166–2177 (2016).
51. Govrin, E.M. & Levine, A. The hypersensitive response facilitates plant infection by the necrotrophic pathogen *Botrytis cinerea*. *Curr. Biol.* **10**, 751–757 (2000).
52. Bos, J.I.B. *et al.* The C-terminal half of *Phytophthora infestans* RXLR effector AVR3a is sufficient to trigger R3a-mediated hypersensitivity and suppress INF1-induced cell death in *Nicotiana benthamiana*. *Plant J.* **48**, 165–176 (2006).
53. Gao, Z., Chung, E.H., Eitas, T.K. & Dangl, J.L. Plant intracellular innate immune receptor resistance to *Pseudomonas syringae pv. maculicola 1* (RPM1) is activated at, and functions on, the plasma membrane. *Proc. Natl. Acad. Sci. USA* **108**, 7619–7624 (2011).
54. Bubeck, D.M., Goodman, M.M., Beavis, W.D. & Grant, D. Quantitative trait loci controlling resistance to gray leaf spot in maize. *Crop Sci.* **33**, 838–847 (1993).
55. Bhuiyan, N.H., Selvaraj, G., Wei, Y. & King, J. Role of lignification in plant defense. *Plant Signal. Behav.* **4**, 158–159 (2009).
56. Tonnessen, B.W. *et al.* Rice phenylalanine ammonia-lyase gene *OsPAL4* is associated with broad spectrum disease resistance. *Plant Mol. Biol.* **87**, 273–286 (2015).
57. Nicholson, R.L. & Hammerschmidt, R. Phenolic compounds and their role in disease resistance. *Annu. Rev. Phytopathol.* **30**, 369–389 (1992).
58. Newman, T.C., Ohme-Takagi, M., Taylor, C.B. & Green, P.J. DST sequences, highly conserved among plant *SAUR* genes, target reporter transcripts for rapid decay in tobacco. *Plant Cell* **5**, 701–714 (1993).
59. Farré, G., Twyman, R.M., Christou, P., Capell, T. & Zhu, C. Knowledge-driven approaches for engineering complex metabolic pathways in plants. *Curr. Opin. Biotechnol.* **32**, 54–60 (2015).
60. König, S. *et al.* Soluble phenylpropanoids are involved in the defense response of *Arabidopsis* against *Verticillium longisporum*. *New Phytol.* **202**, 823–837 (2014).
61. Blount, J.W. *et al.* Altering expression of cinnamic acid 4-hydroxylase in transgenic plants provides evidence for a feedback loop at the entry point into the phenylpropanoid pathway. *Plant Physiol.* **122**, 107–116 (2000).
62. Borrego, E.J. & Kolomiets, M.V. Synthesis and functions of jasmonates in maize. *Plants (Basel)* **5**, E41 (2016).
63. Spoel, S.H., Johnson, J.S. & Dong, X. Regulation of tradeoffs between plant defenses against pathogens with different lifestyles. *Proc. Natl. Acad. Sci. USA* **104**, 18842–18847 (2007).
64. Hirsch, C.N. *et al.* Insights into the maize pan-genome and pan-transcriptome. *Plant Cell* **26**, 121–135 (2014).

ONLINE METHODS

Plant materials. NC292 is a maize inbred line showing strong resistance to SLB, NLB and GLS. It was developed by crossing the resistant inbred NC250 with the widely used inbred line B73, which is moderately susceptible to all three diseases[33]. B73Mdr$_{9.02}$ is a B73 near-isogenic line developed by crossing NC292 to B73, with subsequent backcrossing to B73 and selfing twice, and selection for a multiple disease-resistance locus on bin 9.02 (ref. 29). To fine-map and clone the *qMdr$_{9.02}$* locus, we developed recombinant inbred families from a cross between B73Mdr$_{9.02}$ and B73. An F_2 family of 972 individual plants was generated and selected for recombinants. Recombinants in the *qMdr$_{9.02}$* region were also screened from F_3 (636 plants) and F_4 (309 plants) generations of heterozygous families.

For regional association analysis for SLB, we used 4,413 recombinant inbred lines of the maize nest association mapping population (NAM)[25,32]. We sequenced the *ZmCCoAOMT2* allele from 26 NAM parental lines[31]. To study the molecular mechanism underlying *qMdr$_{9.02}$* mediated quantitative disease resistance, we generated a pair of near-isogenic lines, designated NIL-R and NIL-S, from the fine-mapping process that differed for the *qMdr$_{9.02}$* allele for only a region of ~100-kb.

The maize mutants Mu619 and Mu270 were requested from the Maize Genetics Cooperation Stock Center (URLs). The mutants were originally generated from the UniformMu population by introgressing *Mutator* active lines into the maize inbred line W22 background[65]. The two mutants were crossed to W22 and selfed for two generations to generate the $F_{2:3}$ segregation populations to test for different disease resistance and perform expression experiments.

Field experiments and phenotypic evaluation. In Clayton, North Carolina, USA, plots for SLB trials were planted at 2 m in length with 0.97 m between rows and a 0.6-m alley between ranges. In Andrews, North Carolina, USA, GLS plots were planted as with the SLB trials except with a 4-m plot length. Twelve seeds were planted in each row for SLB trials, whereas 15 seeds per row were planted for GLS trials.

Artificial field inoculation was performed for SLB. SLB inoculum was prepared with *Cochliobolus heterostrophus* isolate 2-16Bm, as previously described[66]. Plants were inoculated at the four- to six-leaf stages by placing approximately 20 SLB-infected sorghum grains in the leaf whorl. GLS was developed by natural infection in Andrews, where there is sufficient natural disease pressure each year.

The days to anthesis (DTA), the number of days between planting and the time at which 50% of the pollen had been shed, was recorded for each row for SLB trials. No DTA data were collected for GLS trials. The rows were scored twice for severity of diseases, approximately 1 week apart in Clayton and 2 weeks apart in Andrews. The SLB and GLS trials were rated with a nine-point scale, with 1 being dead and 9 being the most resistant[10].

The fine-mapping population was planted at Clayton in the summers of 2014 and 2015 for SLB phenotyping. The same population was planted in the summer of 2015 for the GLS test at Andrews. Three replicates were planted for SLB trials, and two replicates were planted for GLS trials. All the mutant families were screened for SLB and GLS in the summers of 2014, 2015 and 2016 at the same locations as those of the fine-mapping population. The transgenic SLB trial plants were planted in Clayton in the summer of 2016.

Growth-chamber experiment and SLB inoculation. A growth chamber of 2.4 × 3.7 × 2.1 m at the North Carolina State University (NCSU) Phytotron was maintained at a temperature of 25 °C during the day and 18 °C during the night, with a 16 h light/8 h dark cycle. Plants were grown in 6-inch pots in standard substrate composed of 1:2 peat-lite/gravel mixture and watered with standard NCSU Phytotron nutrient solution once daily in the afternoon. One seed was planted per pot. A split-split-plot design was used with three replicates for each experiment. Three biological replicates were analyzed for gene expression and lignin quantification experiments, and five biological replicates were prepared for defense-metabolite analysis.

Spray inoculation was carried out at the fifth fully expanded leaf in each experiment. The inoculum consisted of *C. heterostrophus* strain C5 spores suspended in a chilled solution with 0.05% agar and 0.05% Tween-20 in water, with a concentration of 5×10^4 spores/ml. The agar and Tween-20 solution alone was used for mock inoculations. Approximately 0.5 ml of pathogen/mock solutions was evenly sprayed on the leaf with a Paasche H airbrush and a Paasche D200R air compressor set at 23 psi. After they had dried, the plants were placed in clear plastic bags for approximately 18 h to create the free moisture required for spore germination.

Samples were collected at different time points after inoculation, as indicated for each experiment. For gene expression analysis, one leaf punch from the middle of the inoculated leaf was collected, and three plants of each genotype/treatment were pooled and stored at −80 °C. Then, four punches across the center of each leaf were collected for fluorescence microscopy analysis.

Statistical analyses. The disease severity was calculated as the mean of the two ratings for all plots in the SLB and GLS trials. The PROC MIXED procedure in SAS software (v. 9.4; SAS Institute) was used to model each disease separately. LSmeans of each recombinant line were used as the phenotypic values for fine-mapping by fitting line and DTA (only for SLB) as a fixed effect and replication as a random effect. LSmeans for mutants were estimated with genotype and DTA as fixed factors, and replication and year as random factors.

Fine-mapping of *qMdr$_{9.02}$*. SNP genotyping was performed with the KASPar genotyping approach (LGC Genomics) according to the manufacturer's protocol. Public SNPs were selected from MaizeGDB (URLs) on the basis of the physical position on B73 AGPv2. New SNPs were identified by sequencing of PCR products from parental lines B73Mdr$_{9.02}$ and B73. KASP primers for each SNP were developed by LGC Genomics on the basis of the context sequences surrounding the SNP. The PCR assay was set up with a total volume of 5 µl in 384-well plates with both positive and negative controls, according to the recommended touchdown program (LGC Genomics). The fluorescence was detected on a LightCycler 480 instrument (Roche Diagnostics), and the data were analyzed with LightCycler 480 software according to the manufacturer's protocol.

The *qMdr$_{9.02}$* locus was previously identified as a multiple disease-resistance locus conferring quantitative resistance to SLB, NLB and GLS on bin 9.02 (it was previously defined as the 9B locus)[29]. The SNP markers PZA02344 and PZA03416 (**Supplementary Table 2**) in the region were used to screen recombinants from the F_2 population and heterozygous F_3 and F_4 families. The plants with chromosomal recombination between the two markers were selfed and selected for progenies homozygous for the recombination event. Homozygous recombinant progenies were screened for disease resistance to SLB and GLS in the field. Newly developed SNP markers in the *qMdr$_{9.02}$* region (**Supplementary Table 2**) were used to genotype all the recombinants. The *qMdr$_{9.02}$* locus was fine-mapped by comparison of introgression sizes and disease resistance among all the recombinants[67].

Linkage analysis and association analysis of the candidate *qMdr$_{9.02}$* region. First, a joint family linkage analysis was conducted within a linear mixed model framework, in which background genomic effects were accounted for with fixed family mean effects and random line polygenic effects with covariance proportional to a realized relationship matrix, ***G***. Specifically, the model can be described as

$$\mathbf{y} = 1\mu + \mathbf{T}\alpha + \sum_{i=1}^{m} \mathbf{X}_i\beta_i + \mathbf{Zu} + \mathbf{e}$$

where $\boldsymbol{y}$ is the $n \times 1$ vector for the trait values of n NAM RILs, μ is the intercept, $\boldsymbol{T}$ is the $n \times 24$ incidence matrix for the first 24 of the 25 NAM RIL families, and α is the 24×1 vector for family mean effects relative to the reference family, $\boldsymbol{X}_i$ is an $n \times 25$ matrix relating the expected numbers of the non-B73 allele of each RIL at locus i to its corresponding family-specific QTL allele effect, $\boldsymbol{\beta_i}$ is a 25×1 vector for the family-specific QTL effects to be estimated at locus i relative to B73, m is the number of significant marker loci retained in the final model, $\boldsymbol{u}$ is an $n \times 1$ vector of genotype random effects and has covariance structure $var(\mathrm{u}) = \mathbf{G}\sigma_u^2$, where σ_u^2 is the additive genetic variance, $\boldsymbol{G}$ is the realized genomic relationship matrix, $\boldsymbol{Z}$ is a design matrix (identity matrix herein) relating elements of $\boldsymbol{y}$ to elements of $\boldsymbol{u}$, and $\boldsymbol{e}$ is an $n \times 1$ vector of error effects with $\boldsymbol{e} \approx \boldsymbol{N}(\mathbf{0}, \mathbf{I}\sigma_e^2)$.

QTL effects were nested in NAM families to reflect the potential for unique QTL allele effects within each family. A subset of linkage markers significantly associated with the phenotypes was selected by a forward selection approach. The most significant marker (on the basis of an F-test) was selected by conditioning on the selected QTL, covariates and random components of the previous steps until none of the available markers were significant at the Bonferroni corrected type I error rate of 0.05 ($P = 3.4 \times 10^{-5}$). At each step of marker (QTL) selection, the estimated variance components from the last round were held unchanged[68,69].

The QTL allele effects were estimated simultaneously from the final model step. A consensus linkage map consisting of 1,476 markers with a uniform 1-cM intermarker distance was adopted[70].

Second, we used a linear mixed model to scan individual SNPs in the candidate QTL region of chromosome 9, testing whether any SNPs significantly associated with more genetic variation than expected for polygenic background variants. The model can be described as

$$\mathbf{y} = 1\mu + \mathbf{T}\alpha + \sum_{i=1}^{m-1} \mathbf{X}_i\beta_i + \mathbf{w}\gamma + \mathbf{Zu} + \mathbf{e}$$

where $\boldsymbol{w}$ is an $n \times 1$ vector for each Hapmap V3 SNP and sequenced candidate-gene variation within the $qMdr_{9.02}$ region, and γ is the SNP main effect. This model controlled for genome background, other QTL and population main effects to minimize false positive associations. Similarly to the previous model implementation, the variance component was also estimated once with the $m - 1$ QTL included and was held unchanged when each SNP effect was tested.

Isolation of coding sequence and expression analysis of *ZmFBXL*, *ZmCCoAOMT2* and *ZmRLK*. Total RNA was isolated from maize leaf samples with an RNeasy Plant Mini Kit (Qiagen) and treated with RNase-free DNase I (Thermo Fisher Scientific) to remove contaminating DNA, according to the manufacturer's protocol. Complementary DNA (cDNA) was synthesized from 2 µg of total RNA with RevertAid reverse transcriptase (Thermo Fisher Scientific) with random hexamer primers, according to the manufacturer's protocol.

cDNA amplification for *ZmFBXL*, *ZmCCoAOMT2* and *ZmRLK* from B73 and $B73Mdr_{9.02}$ was performed. Primers G1291-1, G9363-1 and G9324-1 (**Supplementary Table 8**) were used to amplify cDNA from candidate genes *ZmFBXL*, *ZmCCoAOMT2* and *ZmRLK* separately with Q5 high-fidelity DNA polymerase (M0491, New England Biolabs).

Primers for quantitative RT–PCR (qRT–PCR) were tested by sequencing standard PCR products to ensure that the correct gene fragments were amplified. qPCR was carried out on a LightCycler 480 Real-Time PCR System (Roche Diagnostics) with SYBR Green Master mix (Applied Biosystems), according to the manufacturer's instructions. qPCR primers for all the studied genes are provided in **Supplementary Table 8**. Gene expression was measured relative to the housekeeping gene *ZmTubulin4*. The $2^{-\Delta Ct}$ (normalized to *ZmTubulin4* expression) or $2^{-\Delta\Delta Ct}$ (normalized to *ZmTubulin4* expression and relative to a specific control) methods were used to calculate relative gene expression. Gene expression for each sample was detected in three technical replicates. Three biological replicates were analyzed for each experiment.

Transgenic functional validation. A 1,548-bp genomic fragment, which includes the *ZmCCoAOMT2* 1,057-bp coding sequence, 450-bp 5′ UTR and 43-bp downstream regions, was amplified from the maize inbred line CML333 with Q5 high-fidelity DNA polymerase (M0491, New England BioLabs). CML333 has the largest QTL effect for SLB resistance at the $qMdr_{9.02}$ locus from the NAM population. The fragment was inserted into the pMCG1005 vector (kindly provided by K. Wang at Iowa State University) under control of the maize ubiquitin promoter. A confirmed clone was designated pMCG1005-ZmCCoMOMT2 and was transformed into the maize inbred line B104 through an *Agrobacterium*-mediated transformation system at the Plant Transformation Facility at Iowa State University. B104 is susceptible to SLB and GLS. All the transformants were selfed or backcrossed to B104.

Transgenic progeny families from six independent transgenic events were generated. Each family was planted in 3 or 4 replicates in Clayton, and each replicate comprised two plots. All the plants were artificially inoculated with SLB inoculums as described above. Individual plants were scored for disease and genotyped. Because B104 is highly susceptible to SLB, the disease develops very rapidly in the B104 background line. The transgenic plants were scored only once when we were able to distinguish the resistant from the susceptible plants. The primer pair G9363-4 (**Supplementary Table 8**), covering one end of the vector and one end of the gene sequence, was used to genotype all the individual plants. Ear height was measured for each plant. The PROC MIXED procedure in SAS software (v. 9.4; SAS Institute) was used to generate LSmeans of each family by fitting genotype and ear height as a fixed effect and replication as a random effect. Tukey's test was used to test for significant differences between genotypes.

Phylogenetic analysis of CCoAOMT. Protein sequences that contained an *S*-adenosylmethionine-dependent methyltransferase domain were obtained from Gramene (URLs) for maize, sorghum and *Arabidopsis*. Phylogenetic-tree construction was performed with the Phylogeny.fr platform (URLs)[71]. Sequence alignments were generated with MUSCLE. Ambiguous regions were removed with Gblocks after alignment. The phylogenetic tree was constructed with the PhyML program. Reliability for internal branching was assessed with the bootstrap method (100 bootstrap replicates). The tree was represented with TreeDyn.

***Arabidopsis* mutant lines and pathogen infection.** We used two T-DNA mutant lines for *AT4G34050*, *ccoaomt1-3* and *ccoaomt1-5*, provided by W. Boerjan[43,72]. *ccoaomt1-3* has an insertion in the fourth exon, whereas *ccoaomt1-5* has an insertion in the third intron. The expression levels of *Arabidopsis CCoAOMT1* were 28 and 84 times lower in *ccoaomt1-3* and *ccoaomt1-5*, respectively, compared with wild-type Columbia (Col-0)[43]. Homozygous mutants were genotyped with the primers shown in **Supplementary Table 8** and selected to evaluate resistance to different pathogens. *rpp4*-mutant plants were used as susceptible controls in the *Hpa* Emwa1 growth assay, and Ws plants were used as a resistance control in the *Hpa* Noco2 growth assay.

Pto DC3000 derivatives containing empty vector or *avrRpt2* were used as bacterial pathogens[73]. Plant inoculations with *Pto* DC3000 and bacterial growth assays were performed as previously described[74]. Three independent experiments were performed. *Hpa* isolates Emwa1 and Noco2 were propagated on the susceptible *Arabidopsis* ecotypes Ws and Col-0, respectively[75]. Plant inoculations with *Hpa* were as previously described[76]. Asexual sporangiophores were counted 7 d after inoculation on a minimum of 40 cotyledons per genotype. Two independent assays were performed and yielded similar results.

CCoAOMT1 expression in Arabidopsis. Microarray gene expression data for *Arabidopsis CCoAOMT1* were downloaded from the TAIR homepage (URLs) from experiments 'AtGenExpress: Pathogen Series:Response to Botrytis cinerea infection', 'AtGenExpress: Pathogen Series:Pseudomonas half leaf injection', 'AtGenExpress: Response to virulent, avirulent, typeIII-secretion system deficient and nonhost bacter', 'AtGenExpress:Response to bacterial-(LPS, HrpZ, Flg22) and oomycete-(NPP1) derived elicitors' and 'AtGenExpress: Pathogen Series: Response to *Erysiphe orontii* infection'[77]. Raw RNA-seq data for *Pto* DC3000 infection of Col-0 seedlings are available in the NCBI Gene Expression Omnibus (GEO) database (URLs) under accession code GSE90606. Experimental details were as described previously[78]. The gene expression results of *Hpa*-infected plants were derived from the data set described by Asai *et al.* (GEO GSE53641)[79].

Metabolite profiling. *Untargeted profiling.* B73, $B73Mdr_{9.02}$, Mu270, Mu619 and W22 plants were used. Ear leaves of the field plants inoculated with *C. heterostrophus* isolate 2-16B were sampled and frozen in liquid nitrogen and stored at –80 °C. Five or six individual plants were pooled together as one sample. Three biological replicates were generated for each genotype. For each sample, 200 mg ground plant tissues was extracted with 1,000 ml 50% (vol/vol) methanol at 60 °C for 30 min. Samples were filtered with a 0.2-µm filter before analysis by LC–MS, as described previously[80]. Metabolites were annotated by searching against the PlantCyc database on the basis of their accurate masses.

Targeted profiling. A pair of near-isogenic lines, NIL-R and NIL-S, that were generated from the fine-mapping process and differed at the ~100-kb *qMdr*$_{9.02}$ region, were used for this experiment. Juvenile-plant growth conditions and SLB inoculation were as described above. Three plants were pooled together as one sample, and five biological replicates were used for analysis. Phytohormones and oxylipins were extracted and analyzed via an LC–MS/MS system[81]. Oxylipin chemical standards were purchased from Larodan and Cayman Chemicals to optimize detection in our system. Multiple reaction monitoring (MRM) transitions for 9,10-EpOM, 9HOT, 12,13-EpOM, 13HOT, 13HOD and cinnamic acid have previously been described[82,83]. The MRM transitions for three oxylipins were determined as 12,13-EpOD (293.2 > 182.9), 9,10,13-THOM (329.2 > 171.1), 9,12,13-THOM (329.2 > 211.2). Metabolites were quantified as compared with deuterated internal standards: dSA, Sigma 736260 for SA; dCA, Sigma 513954 for CA; and dJA, CDN Isotopes D-6936 for oxylipins.

Fluorescence microscopy. Samples were received in 1× PBS and were subsequently processed on an ASP300S tissue processor with multiple stations for a total of 5.25 h. Thereafter, they were embedded in Histoplast LP paraffin (Fisher Healthcare) on edge, and the veins were cut transversely with a HistoStar Embedder (Thermo Scientific). 5-µm sections were taken from fixed leaf punches with a Leica HM-335E microtome and placed onto Fisher Color Frost Plus slides. The slides were depariffinized by two xylene washes for 5 min each and a 100–10% ethanol gradient for 30 s each. Slides received a final rise in nanopure H_2O and were sealed with Molecular Probes ProLong Gold Antifade mountant with Fisher 24 mm × 50 mm no. 1.5 coverglasses. Three biological replicates were analyzed for this experiment. For metabolite analyses, whole inoculated leaves were collected, and samples from three plants were pooled for each genotype/treatment and stored at –80 °C.

Lignin staining was conducted with 0.0025% acriflavine (Sigma A8126) for 15 min, and samples were mounted in 20% glycerol and imaged immediately on a Zeiss LSM880 confocal microscope with a 40× C-Apochromat (NA 1.2), a 488-nm laser line and a 505- to 550-nm emission filter. Lignin was detected via multiphoton excitation on a Zeiss LSM800 confocal microscope with a Coherent Mira 900 Ti:Sapphire laser tuned to 770 nm. Fluorescence spectra between 415 nm and 628 nm were collected, and the lignin autofluorescence (peak emission at 470 nm) was linearly unmixed with Zen 2 or Zen 2012 software. Lignin in the bundle sheaths, xylem and the outer layer of epidermal cells was quantified in FIJI ImageJ, by taking the average peak intensity of a 20-pixel wide-line profile from approximately six different cell-wall locations for each cell type. Data were analyzed and displayed with GraphPad Prism.

Plasmid construction. Plasmids Rp1-D21, ZmHCT:EGFP and G:EGFP were provided by G. Wang[50]. RPM1 p.Asp505Val was provided by J. Dangl. The *ZmCCoAOMT2* gene was cloned from cDNA of B73 or B73Mdr$_{9.02}$. The sequencing-confirmed clones were cloned into the Gateway pDONR207 vector through BP reactions. Subsequently, the confirmed clones were transferred into the vector G257 through LR reactions. Primers used for generating the constructs are listed in **Supplementary Table 8**.

***Agrobacterium*-mediated transient expression in *N. benthamiana*.** *A. tumefaciens* strain GV3101 was used in molecular cloning experiments. Recombinant *A. tumefaciens* stains containing different binary plasmids were grown as previously described with appropriate antibiotics[50]. Agroinfiltration experiments were performed on 4- to 6-week-old *N. benthamiana*–infected plants. To enhance the expression of the transiently expressed target gene, a vector containing the silencing suppressor p19 from tomato bushy stunt virus was used[84]. Transient coexpression was performed as follows. The *A. tumefaciens* strains carrying the respective plasmids were mixed in induction buffer (10 mM MES, pH 5.6, 10 mM $MgCl_2$ and 200 µM acetosyringone) to a final OD_{600} of 0.5 for Rp1-D21, 0.2 for p19, 0.3 for RPM1 (p.Asp505Val) and 0.4 for all other constructs. All suspensions were incubated for 1–3 h before infiltration into the abaxial side of *N. benthamiana*–infected leaves. After infiltration, plants were kept at room temperature under a 16-h light/8-h dark cycle. At least seven individual leaves were infiltrated, and each leaf had four infiltration sites per construct (**Supplementary Fig. 15**). Symptom development was recorded from 1–4 d after infiltration[52]. GUS protein was used as a negative control. The positive control was the ZmHCT (hydroxycinnamoyltransferase) protein, which has previously been shown to effectively suppress Rp1-D21-mediated cell death[85].

Data availability. Genomic DNA sequences for *ZmCCoAOMT2* from the 26 parental lines of NAM and for NC250 can be found in the NCBI database under accession numbers KY556584 through KY556610. cDNA sequences of *ZmFBXL* and *ZmRLK* from B73 and NC250 are available under accession numbers KY556611 through KY556614.

65. McCarty, D.R. *et al.* Steady-state transposon mutagenesis in inbred maize. *Plant J.* **44**, 52–61 (2005).
66. Carson, M.L., Stuber, C.W. & Senior, M.L. Identification and mapping of quantitative trait loci conditioning resistance to southern leaf blight of maize caused by *Cochliobolus heterostrophus* race O. *Phytopathology* **94**, 862–867 (2004).
67. Yang, Q., Zhang, D. & Xu, M. A sequential quantitative trait locus fine-mapping strategy using recombinant-derived progeny. *J. Integr. Plant Biol.* **54**, 228–237 (2012).
68. Kang, H.M. *et al.* Variance component model to account for sample structure in genome-wide association studies. *Nat. Genet.* **42**, 348–354 (2010).
69. Zhang, Z. *et al.* Mixed linear model approach adapted for genome-wide association studies. *Nat. Genet.* **42**, 355–360 (2010).
70. Bian, Y. & Holland, J.B. Ensemble learning of QTL models improves prediction of complex traits. *G3 (Bethesda)* **5**, 2073–2084 (2015).
71. Dereeper, A. *et al.* Phylogeny.fr: robust phylogenetic analysis for the non-specialist. *Nucleic Acids Res.* **36**, W465–W469 (2008).
72. Alonso, J.M. *et al.* Genome-wide insertional mutagenesis of *Arabidopsis thaliana*. *Science* **301**, 653–657 (2003).
73. Hubert, D.A., He, Y., McNulty, B.C., Tornero, P. & Dangl, J.L. Specific *Arabidopsis* HSP90.2 alleles recapitulate RAR1 cochaperone function in plant NB-LRR disease resistance protein regulation. *Proc. Natl. Acad. Sci. USA* **106**, 9556–9563 (2009).
74. Tornero, P. & Dangl, J.L. A high-throughput method for quantifying growth of phytopathogenic bacteria in *Arabidopsis thaliana*. *Plant J.* **28**, 475–481 (2001).
75. Holt, B.F. III *et al.* An evolutionarily conserved mediator of plant disease resistance gene function is required for normal *Arabidopsis* development. *Dev. Cell* **2**, 807–817 (2002).
76. Mukhtar, M.S. *et al.* Independently evolved virulence effectors converge onto hubs in a plant immune system network. *Science* **333**, 596–601 (2011).
77. Winter, D. *et al.* An "Electronic Fluorescent Pictograph" browser for exploring and analyzing large-scale biological data sets. *PLoS One* **2**, e718 (2007).
78. Yang, L. *et al. Pseudomonas syringae* type III effector HopBB1 promotes host transcriptional repressor degradation to regulate phytohormone responses and virulence. *Cell Host Microbe* **21**, 156–168 (2017).
79. Asai, S. *et al.* Expression profiling during *Arabidopsis*/downy mildew interaction reveals a highly-expressed effector that attenuates responses to salicylic acid. *PLoS Pathog.* **10**, e1004443 (2014).
80. Strauch, R.C., Svedin, E., Dilkes, B., Chapple, C. & Li, X. Discovery of a novel amino acid racemase through exploration of natural variation in *Arabidopsis thaliana*. *Proc. Natl. Acad. Sci. USA* **112**, 11726–11731 (2015).
81. Christensen, S.A. *et al.* The novel monocot-specific 9-lipoxygenase ZmLOX12 is required to mount an effective jasmonate-mediated defense against *Fusarium verticillioides* in maize. *Mol. Plant Microbe Interact.* **27**, 1263–1276 (2014).
82. Ludovici, M. *et al.* Quantitative profiling of oxylipins through comprehensive LC-MS/MS analysis of *Fusarium verticillioides* and maize kernels. *Food Addit. Contam. Part A Chem. Anal. Control Expo. Risk Assess.* **31**, 2026–2033 (2014).
83. Pan, X., Welti, R. & Wang, X. Quantitative analysis of major plant hormones in crude plant extracts by high-performance liquid chromatography-mass spectrometry. *Nat. Protoc.* **5**, 986–992 (2010).
84. Voinnet, O., Rivas, S., Mestre, P. & Baulcombe, D. An enhanced transient expression system in plants based on suppression of gene silencing by the p19 protein of tomato bushy stunt virus. *Plant J.* **33**, 949–956 (2003).
85. Wang, G. *et al.* Maize homologs of HCT, a key enzyme in lignin biosynthesis, bind the NLR Rp1 proteins to modulate the defense response. *Plant Physiol.* **171**, 2166–2177 (2015).

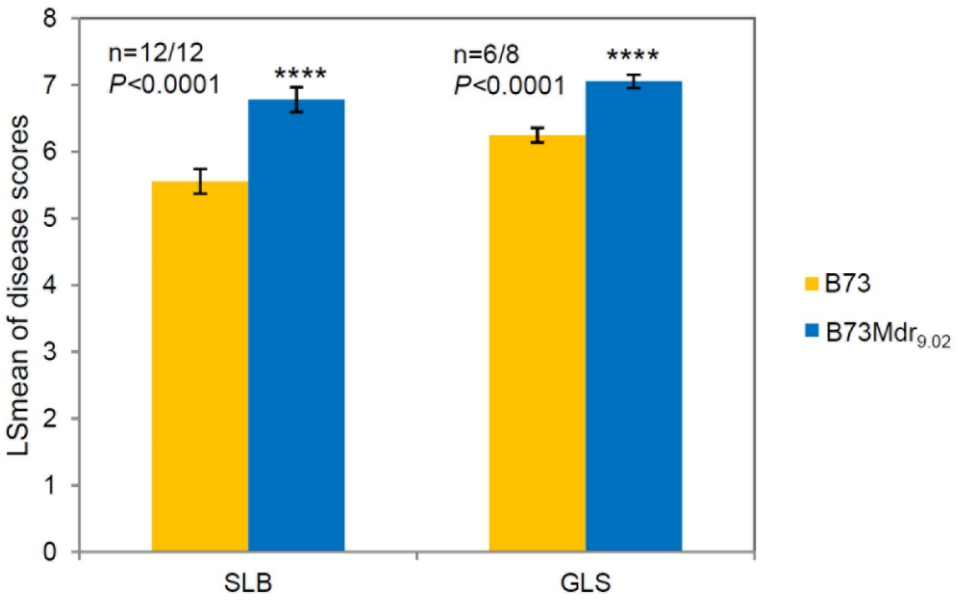

Supplementary Figure 1

Comparison of field disease resistance between B73Mdr$_{9.02}$ and B73 for SLB and GLS.

The disease resistance was rated using a nine-point scale with 1 being dead and 9 being the most resistant. Least square means of SLB and GLS are shown in the bar chart. Error bars indicate standard error of the LSmeans. B73Mdr$_{9.02}$ is more resistant to SLB and GLS than B73 in the field. Tukey's test (two-tailed) indicates a significant difference. ****$P < 0.0001$. Number of plots for each genotype of each disease is indicated above the corresponding columns.

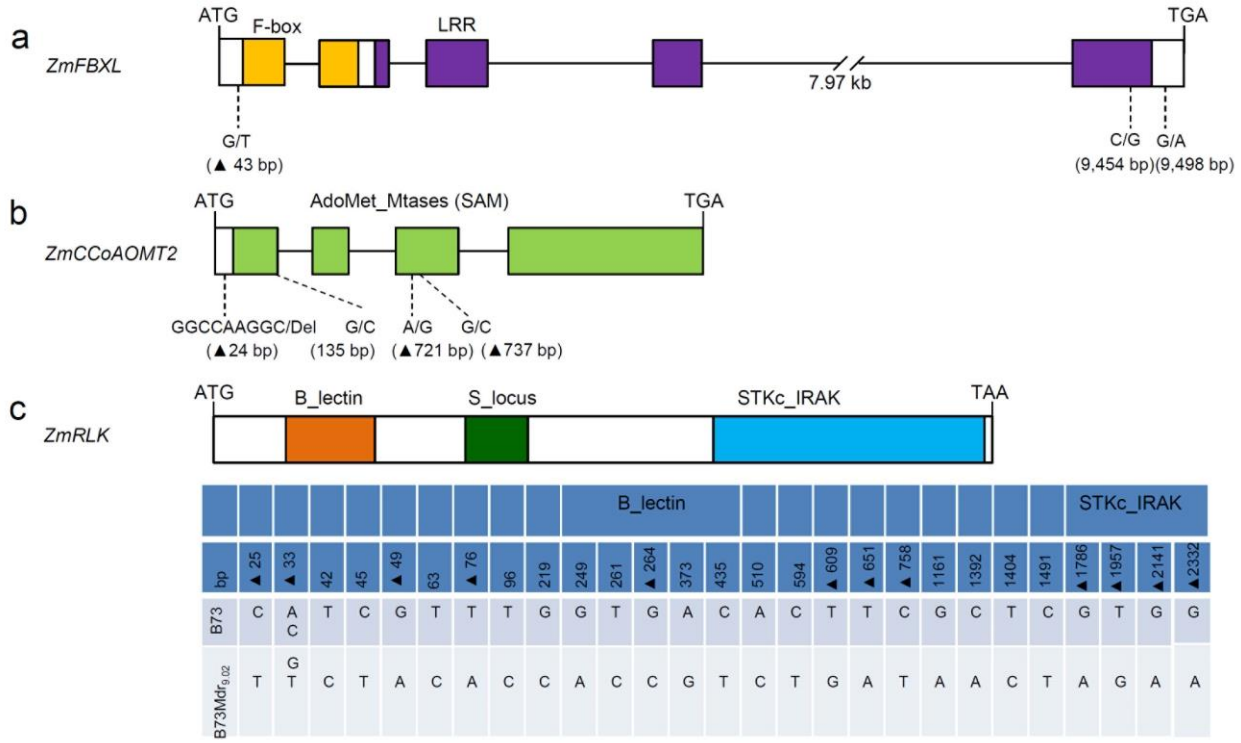

Supplementary Figure 2

Gene structure, protein-domain prediction and polymorphic sites in the coding region of the three candidate genes between B73 and B73Mdr$_{9.02}$.

(a) Gene structure of *ZmFBXL*. (b) Gene structure of *ZmCCoAOMT2*. (c) Gene structure of *ZmRLK*. Exons are indicated as rectangle bars, and introns as black lines between exons. Predicted domains are indicated in different colors while white portion of each rectangle represents coding region with no predicted domain. Start and stop codon of each gene was indicated. LRR, leucine-rich repeat; AdoMet_Mtases (SAM), S-adenosylmethionine-dependent methyltransferases; B_lectin, Bulb-type mannose-specific lectin; S_locus, S_locus glycoprotein domain; STKc_IRAK, catalytic domain of the Serine/Threonine kinases, Interleukin-1 Receptor Associated Kinases. Polymorphic sites are positioned relative to the start codon of the B73 allele, and nonsynonymous SNPs are labeled with a black triangle.

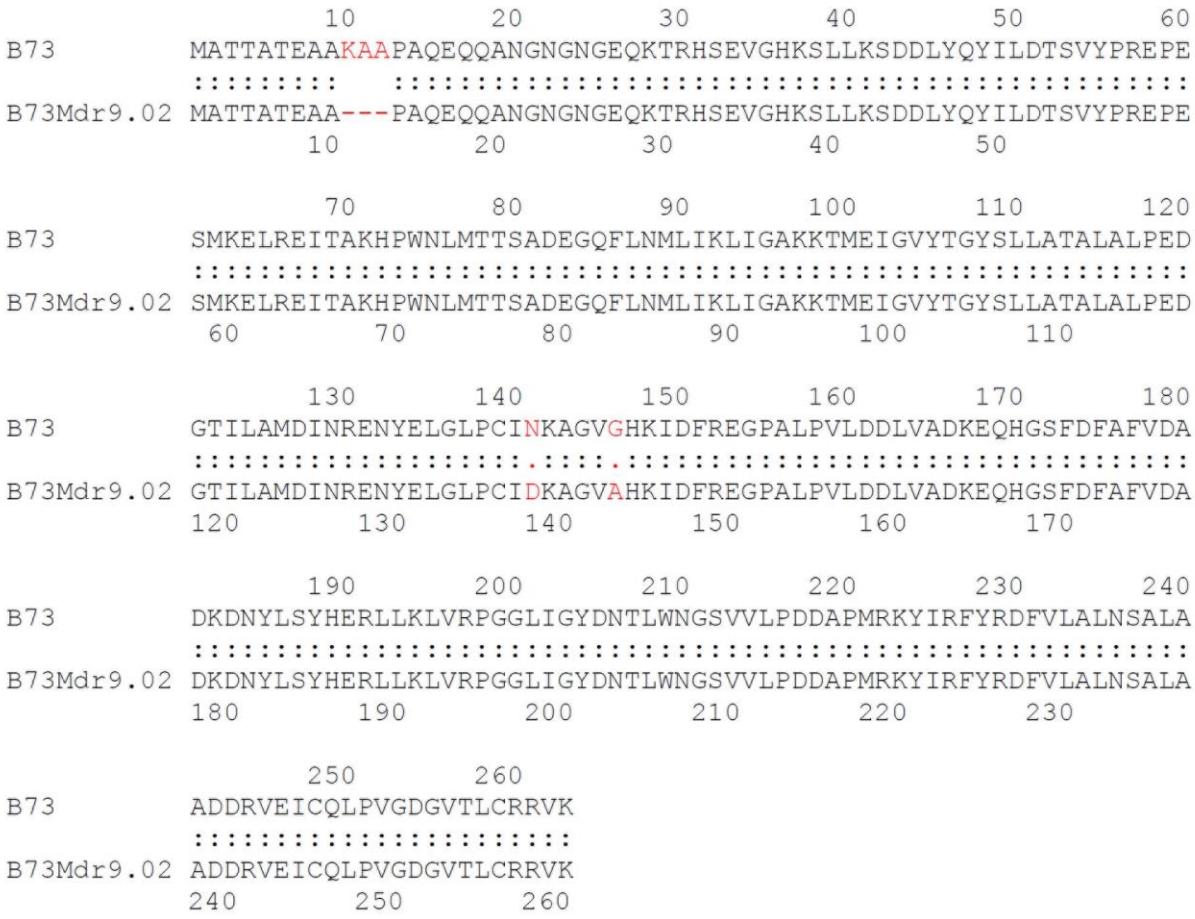

Supplementary Figure 3

Comparison of deduced amino acid sequences of ZmCCoAOMT2 between B73 and B73Mdr$_{9.02}$.

```
B73Mdr9.02    MATTATE----AAPAQEQQANG--NGNGEQKTRHSEVGHKSLLKSDDLYQNDPQYILDTSVYPREPE
B73           MATTATEAAK-AAPAQEQQANG--NGNGEQKTRHSEVGHKSLLKSDDLYQNDPQYILDTSVYPREPE
Oh7b          MATTATEAAK-AAPAQEQQANG--NGNGEQKTRHSEVGHKSLLKSDDLYQ----YILDTSVYPREPE
B97           MATTATEATKTAAPAQEQQANSNGNGNGEQKTRHSEVGHKSLLKSDDLYQ----YILDTSVYPREPE
M162W         MATTATEAAK-AAPAQEQQANG--NGNGEQKTRHSEVGHKSLLKSDDLYQ----YILDTSVYPREPE
Ms71          MATTATEATKTTAPAQEQQANGNGNGNGEQKTRHSEVGHKSLLKSDDLYQ----YILDTSVYPREPE
Tx303         MATTATEAAK-AAPAQEQQANG--NGNGEQKTRHSEVGHKSLLKSDDLYQ----YILDTSVYPREPE
Tzi8          MATTATE----AAPAQEQQANG--NGNGEQKTRHSEVGHKSLLKSDDLYQ----YILDTSVYPREPE
Ky21          MATTATEATKTTAPAQEQQANGNGNGNGEQKTRHSEVGHKSLLKSDDLYQ----YILDTSVYPREPE
Ki3           MATTATEATKTTAPAQEQQANGNGNGNGEQKTRHSEVGHKSLLKSDDLYQ----YILDTSVYPREPE
Il14H         MATTATEAAK-AAPAQEQQANG--NGNGEQKTRHSEVGHKSLLKSDDLYQ----YILDTSVYPREPE
CML69         MATTATEATKTTAPAQEQQANGNGNGNGEQKTRHSEVGHKSLLKSDDLYQ----YILDTSVYPREPE
P39           MATTATEAAK-AAPAQEQQANG--NGNGEQKTRHSEVGHKSLLKSDDLYQ----YILDTSVYPREPE
CML52         MATTATEATKTTAPAQEQQANG--NGNGEQKTRHSEVGHKSLLKSDDLYQ----YILDTSVYPREPE
Oh43          MATTAT---KTTAPAQEQQANG--NGNGEQKTRHSEVGHKSLLKSDDLYQ----YILDTSVYPREPE
CML277        MATTATEATK-AAPAQEQQANG--NGNGEQKTRHSEVGHKSLLKSDDLYQ----YILDTSVYPREPE
NC358         MATTATEATKTAAPAQEQQANSNGNGNGEQKTRHSEVGHKSLLKSDDLYQ----YILDTSVYPREPE
Mo18W         MATTATEATKTTAPAQEQQANGNGNGNGEQKTRHSEVGHKSLLKSDDLYQ----YILDTSVYPREPE
CML228        MATTATEATKTTAPAQEQQANGNGNGNGEQKTRHSEVGHKSLLKSDDLYQ----YILDTSVYPREPE
```

```
NC350      MATTAT---KTTAPAQEQQANG--NGNGEQKTRHSEVGHKSLLKSDDLYQ----YILDTSVYPREPE
M37W       MATTATEATKTTAPAQEQQANG--NGNGEQKTRHSEVGHKSLLKSDDLYQ----YILDTSVYPREPE
CML322     MATTATEATKTTAPAQEQQANGNGNGNGEQKTRHSEVGHKSLLKSDDLYQ----YILDTSVYPREPE
CML247     MATTATE----AAPAQEQQANG--NGNGEQKTRHSEVGHKSLLKSDDLYQ----YILDTSVYPREPE
Ki11       MATTATEATKTTAPAQEQQANGNGNGNGEQKTRHSEVGHKSLLKSDDLYQ----YILDTSVYPREPE
CML103     MATTATEATK-AAPAQEQQANG--NGNGEQKTRHSEVGHKSLLKSDDLYQ----YILDTSVYPREPE
Hp301      MATTAT---KTTAPAQEQQANG--NGNGEQKTRHSEVGHKSLLKSDDLYQ----YILDTSVYPREPE
CML333     MATTAT---KTTAPAQEQQANG--NGNGEQKTRHSEVGHKSLLKSDDLYQ----YILDTSVYPREPE

cons       ******:     *********.    ************************    *************


B73Mdr9.02 SMKELREITAKHPWNLMTTSADEGQFLNMLIKLIGAKKTMEIGVYTGYSLLATALALPEDGTILAMDIN
B73        SMKELREITAKHPWNLMTTSADEGQFLNMLIKLIGAKKTMEIGVYTGYSLLATALALPEDGTILAMDIN
Oh7b       SMKELREITAKHPWNLMTTSADEGQFLNMLIKLIGAKKTMEIGVYTGYSLLATALALPEDGTILAMDIN
B97        SMKELREITAKHPWNLMTTSADEGQFLNMLIKLIGAKKTMEIGVYTGYSLLATALALPEDGTILAMDIN
M162W      SMKELREITAKHPWNLMTTSADEGQFLNMLIKLIGAKKTMEIGVYTGYSLLATALALPEDGTILAMDIN
Ms71       SMKELREITAKHPWNLMTTSADEGQFLNMLIKLIGAKKTMEIGVYTGYSLLATALALPEDGTILAMDIN
Tx303      SMKELREITAKHPWNLMTTSADEGQFLNMLIKLIGAKKTMEIGVYTGYSLLATALALPEDGTILAMDIN
Tzi8       SMKELREITAKHPWNLMTTSADEGQFLNMLIKLIGAKKTMEIGVYTGYSLLATALALPEDGTILAMDIN
Ky21       SMKELREITAKHPWNLMTTSADEGQFLNMLIKLIGAKKTMEIGVYTGYSLLATALALPEDGTILAMDIN
Ki3        SMKELREITAKHPWNLMTTSADEGQFLNMLIKLIGAKKTMEIGVYTGYSLLATALALPEDGTILAMDIN
Il14H      SMKELREITAKHPWNLMTTSADEGQFLNMLIKLIGAKKTMEIGVYTGYSLLATALALPEDGTILAMDIN
CML69      SMKELREITAKHPWNLMTTSADEGQFLNMLIKLIGAKKTMEIGVYTGYSLLATALALPEDGTILAMDIN
P39        SMKELREITAKHPWNLMTTSADEGQFLNMLIKLIGAKKTMEIGVYTGYSLLATALALPEDGTILAMDIN
CML52      SMKELREITAKHPWNLMTTSADEGQFLNMLIKLIGAKKTMEIGVYTGYSLLATALALPEDGTILAMDIN
Oh43       SMKELREITAKHPWNLMTTSADEGQFLNMLIKLIGAKKTMEIGVYTGYSLLATALALPEDGTILAMDIN
CML277     SMKELREITAKHPWNLMTTSADEGQFLNMLIKLIGAKKTMEIGVYTGYSLLATALALPEDGTILAMDIN
NC358      SMKELREITAKHPWNLMTTSADEGQFLNMLIKLIGAKKTMEIGVYTGYSLLATALALPEDGTILAMDIN
Mo18W      SMKELREITAKHPWNLMTTSADEGQFLNMLIKLIGAKKTMEIGVYTGYSLLATALALPEDGTILAMDIN
CML228     SMKELREITAKHPWNLMTTSADEGQFLNMLIKLIGAKKTMEIGVYTGYSLLATALALPEDGTILAMDIN
NC350      SMKELREITAKHPWNLMTTSADEGQFLNMLIKLIGAKKTMEIGVYTGYSLLATALALPEDGTILAMDIN
M37W       SMKELREITAKHPWNLMTTSADEGQFLNMLIKLIGAKKTMEIGVYTGYSLLATALALPEDGTILAMDIN
CML322     SMKELREITAKHPWNLMTTSADEGQFLNMLIKLIGAKKTMEIGVYTGYSLLATALALPEDGTILAMDIN
CML247     SMKELREITAKHPWNLMTTSADEGQFLNMLIKLIGAKKTMEIGVYTGYSLLATALALPEDGTILAMDIN
Ki11       SMKELREITAKHPWNLMTTSADEGQFLNMLIKLIGAKKTMEIGVYTGYSLLATALALPEDGTILAMDIN
CML103     SMKELREITAKHPWNLMTTSADEGQFLNMLIKLIGAKKTMEIGVYTGYSLLATALALPEDGTILAMDIN
Hp301      SMKELREITAKHPWNLMTTSADEGQFLNMLIKLIGAKKTMEIGVYTGYSLLATALALPEDGTILAMDIN
CML333     SMKELREITAKHPWNLMTTSADEGQFLNMLIKLIGAKKTMEIGVYTGYSLLATALALPEDGTILAMDIN

cons       **********************************************************************


B73Mdr9.02 RENYELGLPCIDKAGVAHKIDFREGPALPVLDDLVADKEQHGSFDFAFVDADKDNYLSYHERLLKLVRP
B73        RENYELGLPCINKAGVGHKIDFREGPALPVLDDLVADKEQHGSFDFAFVDADKDNYLSYHERLLKLVRP
Oh7b       RENYELGLPCINKAGVGHKIDFREGPALPVLDDLVADKEQHGSFDFAFVDADKDNYLSYHERLLKLVRP
B97        RENYELGLPCINKAGVGHKIDFREGPALPVLDDLVADKEQHGSFDFAFVDADKDNYLSYHERLLKLVRP
M162W      RENYELGLPCINKAGVGHKIDFREGPALPVLDDLVADKEQHGSFDFAFVDADKDNYLSYHERLLKLVRP
Ms71       RENYELGLPCINKAGVGHKIDFREGPALPVLDDLVADKEQHGSFDFAFVDADKDNYLSYHERLLKLVRP
Tx303      RENYELGLPCINKAGVGHKIDFREGPALPVLDDLVADKEQHGSFDFAFVDADKDNYLSYHERLLKLVRP
Tzi8       RENYELGLPCINKAGVGHKIDFREGPALPVLDDLVADKEQHGSFDFAFVDADKDNYLSYHERLLKLVRP
Ky21       RENYELGLPCINKAGVGHKIDFREGPALPVLDDLVADKEQHGSFDFAFVDADKDNYLNYHERLLKLVRP
Ki3        RENYELGLPCINKAGVGHKIDFREGPALPVLDDLVADKEQHGSFDFAFVDADKDNYLSYHERLLKLVRP
Il14H      RENYELGLPCINKAGVGHKIDFREGPALPVLDDLVADKEQHGSFDFAFVDADKDNYLSYHERLLKLVRP
CML69      RENYELGLPCINKAGVGHKIDFREGPALPVLDDLVADKEQHGSFDFAFVDADKDNYLNYHERLLKLVRP
```

```
P39          RENYELGLPCINKAGVGHKIDFREGPALPVLDDLVADKEQHGSFDFAFVDADKDNYLSYHERLLKLVRP
CML52        RENYELGLPCINKAGVGHKIDFREGPALPVLDDLVADKEQHGSFDFAFVDADKDNYLNYHERLLKLVRP
Oh43         RENYELGLPCINKAGVGHKIDFREGPALPVLDDLVADKEQHGSFDFAFVDADKDNYLSYHERLLKLVRP
CML277       RENYELGLPCIDKAGVAHKIDFREGPALPVLDDLVADKEQHGSFDFAFVDADKDNYLNYHERLLKLVRP
NC358        RENYELGLPCINKAGVGHKIDFREGPALPVLDDLVADKEQHGSFDFAFVDADKDNYLSYHERLLKLVRP
Mo18W        RENYELGLPCINKAGVGHKIDFREGPALPVLDDLVADKEQHGSFDFAFVDADKDNYLSYHERLLKLVRP
CML228       RENYELGLPCINKAGVGHKIDFREGPALPVLDDLVADKEQHGSFDFAFVDADKDNYLSYHERLLKLVRP
NC350        RENYELGLPCINKAGVGHKIDFREGPALPVLDDLVADKEQHGSFDFAFVDADKDNYLSYHERLLKLVRP
M37W         RENYELGLPCINKAGVGHKIDFREGPALPVLDDLVADKEQHGSFDFAFVDADKDNYLSYHERLLKLVRP
CML322       RENYELGLPCINKAGVGHKIDFREGPALPVLDDLVADKEQHGSFDFAFVDADKDNYLSYHERLLKLVRP
CML247       RENYELGLPCINKAGVGHKIDFREGPALPVLDDLVADKEQHGSFDFAFVDADKDNYLSYHERLLKLVRP
Ki11         RENYELGLPCINKAGVGHKIDFREGPALPVLDDLVADKEQHGSFDFAFVDADKDNYLSYHERLLKLVRP
CML103       RENYELGLPCINKAGVGHKIDFREGPALPVLDDLVADKEQHGSFDFAFVDADKDNYLSYHERLLKLVRP
Hp301        RENYELGLPCINKAGVGHKIDFREGPALPVLDDLVADKEQHGSFDFAFVDADKDNYLSYHERLLKLVRP
CML333       RENYELGLPCINKAGVGHKIDFREGPALPVLDDLVADKEQHGSFDFAFVDADKDNYLSYHERLLKLVRP

cons         ***********:****.****************************************.***********

B73Mdr9.02   GGLIGYDNTLWNGSVVLPDDAPMRKYIRFYRDFVLALNSALAADDRVEICQLPVGDGVTLCRRVK
B73          GGLIGYDNTLWNGSVVLPDDAPMRKYIRFYRDFVLALNSALAADDRVEICQLPVGDGVTLCRRVK
Oh7b         GGLIGYDNTLWNGSVVLPDDAPMRKYIRFYRDFVLALNSALAADDRVEICQLPVGDGVTLCRRVK
B97          GGLIGYDNTLWNGSVVLPDDAPMRKYIRFYRDFVLALNSALAADDRVEICQLPVGDGVTLCRRVK
M162W        GGLIGYDNTLWNGSVVLPDDAPMRKYIRFYRDFVLALNSALAADDRVEICQLPVGDGVTLCRRVK
Ms71         GGLIGYDNTLWNGSVVLPDDAPMRKYIRFYRDFVLALNSALAADDRVEICQLPVGDGVTLCRRVK
Tx303        GGLIGYDNTLWNGSVVLPDDAPMRKYIRFYRDFVLALNSALAADDRVEICQLPVGDGVTLCRRVK
Tzi8         GGLIGYDNTLWNGSVVLPDDAPMRKYIRFYRDFVLALNSALAADDRVEICQLPVGDGVTLCRRVK
Ky21         GGLIGYDNTLWNGSVVLPDDAPMRKYIRFYRDFVLALNSALAADDRVEICQLPVGDGVTLCRRVK
Ki3          GGLIGYDNTLWNGSVVLPDDAPMRKYIRFYRDFVLALNSALAADDRVEICQLPVGDGVTLCRRVK
Il14H        GGLIGYDNTLWNGSVVLPDDAPMRKYIRFYRDFVLALNSALAADDRVEICQLPVGDGVTLCRRVK
CML69        GGLIGYDNTLWNGSVVLPDDAPMRKYIRFYRDFVLALNSALAADDRVEICQLPVGDGVTLCRRVK
P39          GGLIGYDNTLWNGSVVLPDDAPMRKYIRFYRDFVLALNSALAADDRVEICQLPVGDGVTLCRRVK
CML52        GGLIGYDNTLWNGSVVLPDDAPMRKYIRFYRDFVLALNSALAADDRVEICQLPVGDGVTLCRRVK
Oh43         GGLIGYDNTLWNGSVVLPDDAPMRKYIRFYRDFVLALNSALAADDRVEICQLPVGDGVTLCRRVK
CML277       GGLIGYDNTLWNGSVVLPDDAPMRKYIRFYRDFVLALNSALAADDRVEICQLPVGDGVTLCRRVK
NC358        GGLIGYDNTLWNGSVVLPDDAPMRKYIRFYRDFVLALNSALAADDRVEICQLPVGDGVTLCRRVK
Mo18W        GGLIGYDNTLWNGSVVLPDDAPMRKYIRFYRDFVLALNSALAADDRVEICQLPVGDGVTLCRRVK
CML228       GGLIGYDNTLWNGSVVLPDDAPMRKYIRFYRDFVLALNSALAADDRVEICQLPVGDGVTLCRRVK
NC350        GGLIGYDNTLWNGSVVLPDDAPMRKYIRFYRDFVLALNSALAADDRVEICQLPVGDGVTLCRRVK
M37W         GGLIGYDNTLWNGSVVLPDDAPMRKYIRFYRDFVLALNSALAADDRVEICQLPVGDGVTLCRRVK
CML322       GGLIGYDNTLWNGSVVLPDDAPMRKYIRFYRDFVLALNSALAADDRVEICQLPVGDGVTLCRRVK
CML247       GGLIGYDNTLWNGSVVLPDDAPMRKYIRFYRDFVLALNSALAADDRVEICQLPVGDGVTLCRRVK
Ki11         GGLIGYDNTLWNGSVVLPDDAPMRKYIRFYRDFVLALNSALAADDRVEICQLPVGDGVTLCRRVK
CML103       GGLIGYDNTLWNGSVVLPDDAPMRKYIRFYRDFVLALNSALAADDRVEICQLPVGDGVTLCRRVK
Hp301        GGLIGYDNTLWNGSVVLPDDAPMRKYIRFYRDFVLALNSALAADDRVEICQLPVGDGVTLCRRVK
CML333       GGLIGYDNTLWNGSVVLPDDAPMRKYIRFYRDFVLALNSALAADDRVEICQLPVGDGVTLCRRVK

cons         ************************************************************
```

Supplementary Figure 4

Comparison of deduced amino acid sequences of ZmCCoAOMT2 among 26 NAM founder lines and $B73Mdr_{9.02.}$

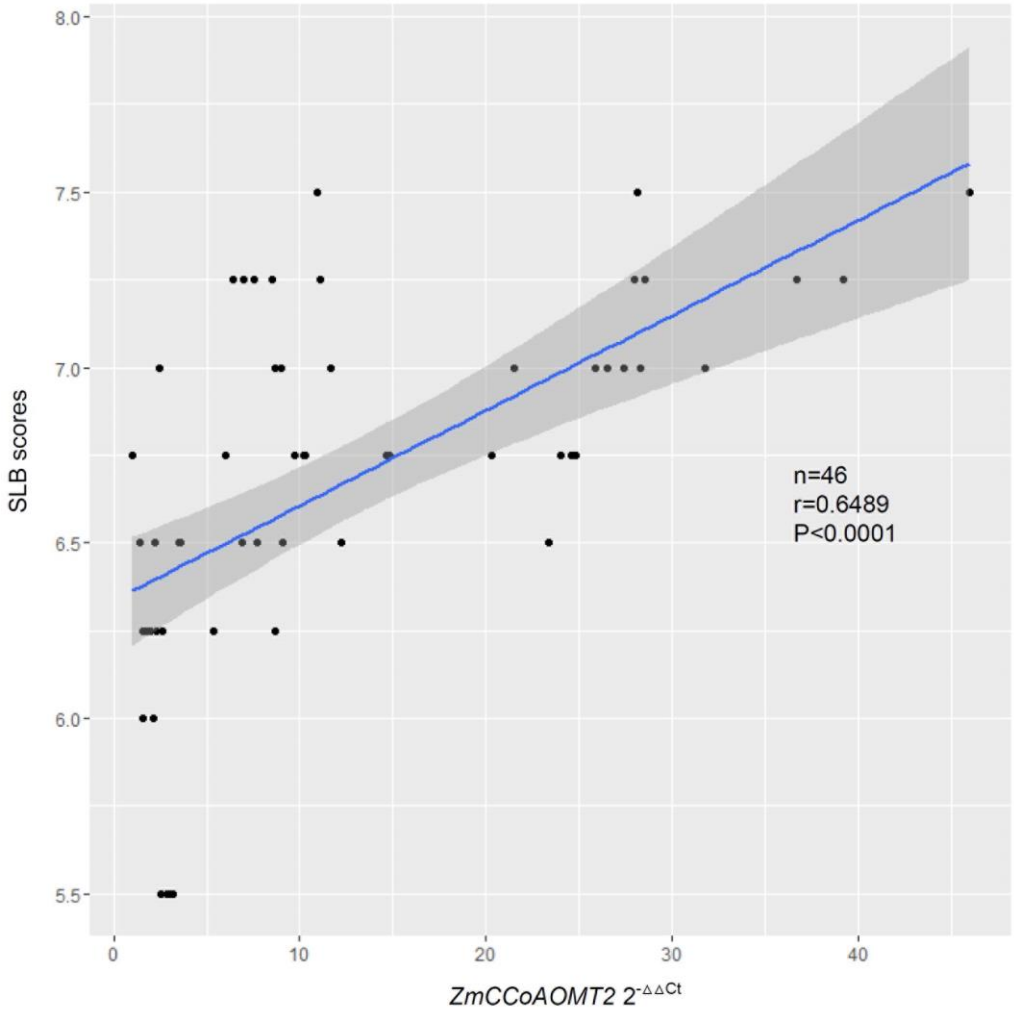

Supplementary Figure 5

Pearson's correlation coefficient between *ZmCCoAOMT2* transcript levels and SLB resistance in transgenic plants.

A total of 46 T_1 individual plants were included. The disease resistance was rated using a nine-point scale with 1 being dead and 9 being the most resistant. *ZmCCoAOMT2* expression is significantly positively correlated with SLB resistance in the field. Darker shading indicates the 95% confidence level interval. $n = 46$ individual plants. $r = 0.6489$ with $P < 0.0001$.

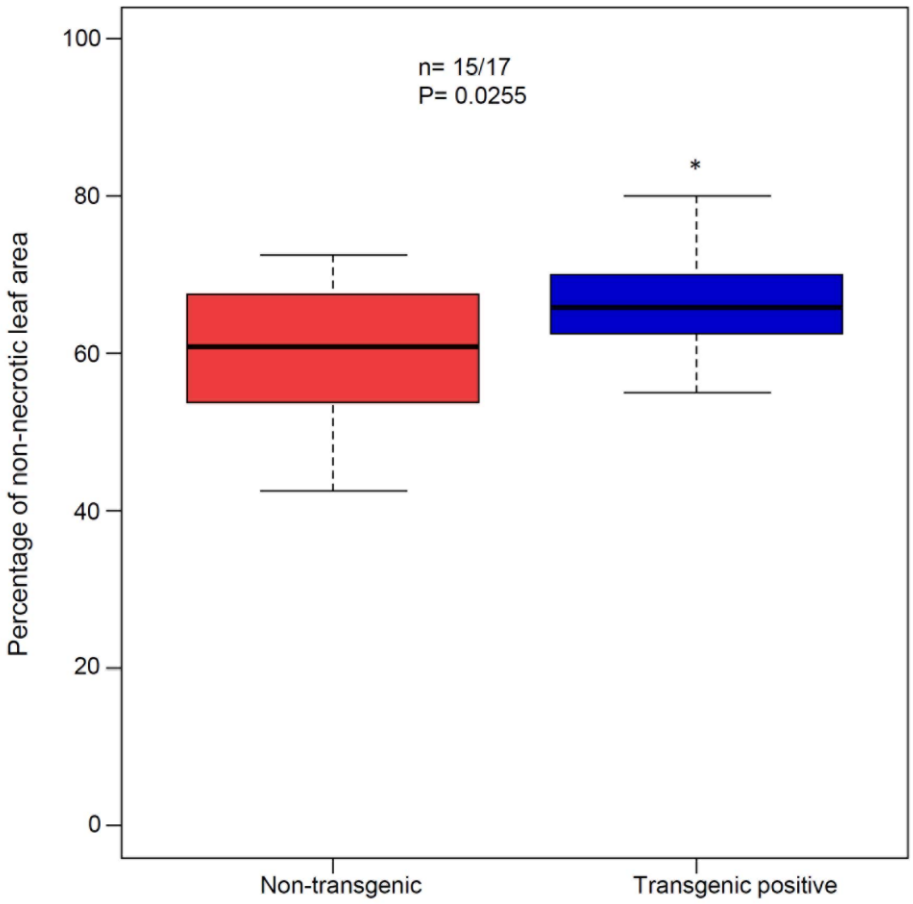

Supplementary Figure 6

Box-and-whisker plot showing percentage of non-necrotic leaf area of SLB infection on T_2 backcrossed transgenic juvenile plants from event A693B5 in growth chamber.

Center line marks median. The bottom and top edges of the boxes indicate the 25th and 75th percentiles. Whiskers mark the range of the data excluding outliers. Number of samples for each genotype is indicated. The *P* values reflect results obtained from unpaired two-tailed t-tests between non-transgenic and transgenic positive plants. *n* is the number of plants in non-transgenic/transgenic positive groups.

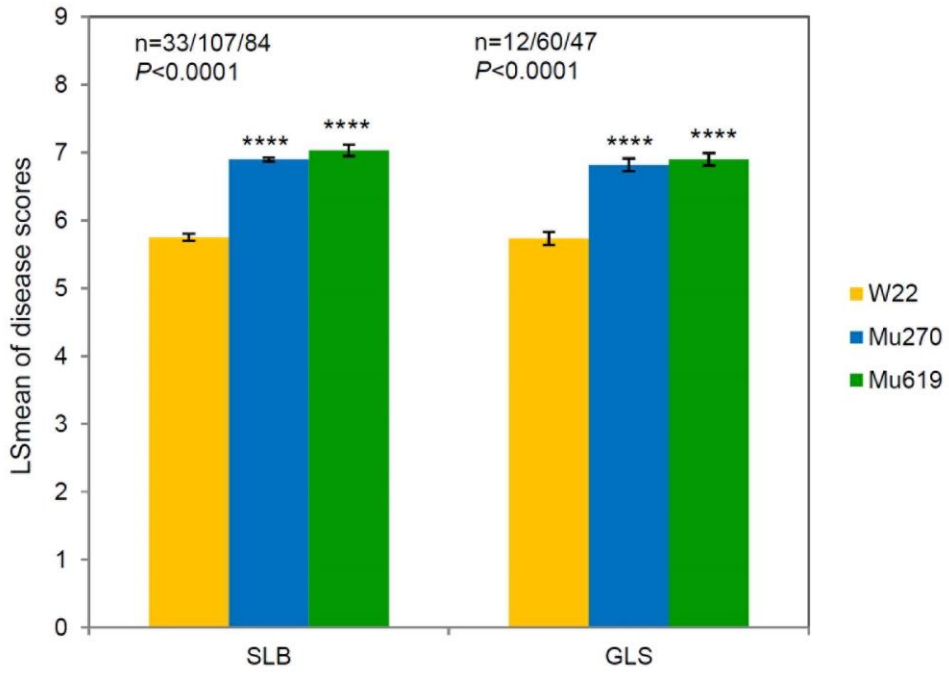

Supplementary Figure 7

Disease levels of two *Mutator*-insertion lines and W22 in the field.

The disease resistance was rated using a nine-point scale with 1 being dead and 9 being the most resistant. Number of plots for each genotype of each disease is indicated above the corresponding columns. Bars indicate standard error of the LSmeans. Tukey's test (two-tailed) indicates a significant difference between insertion line and W22. ****$P < 0.0001$.

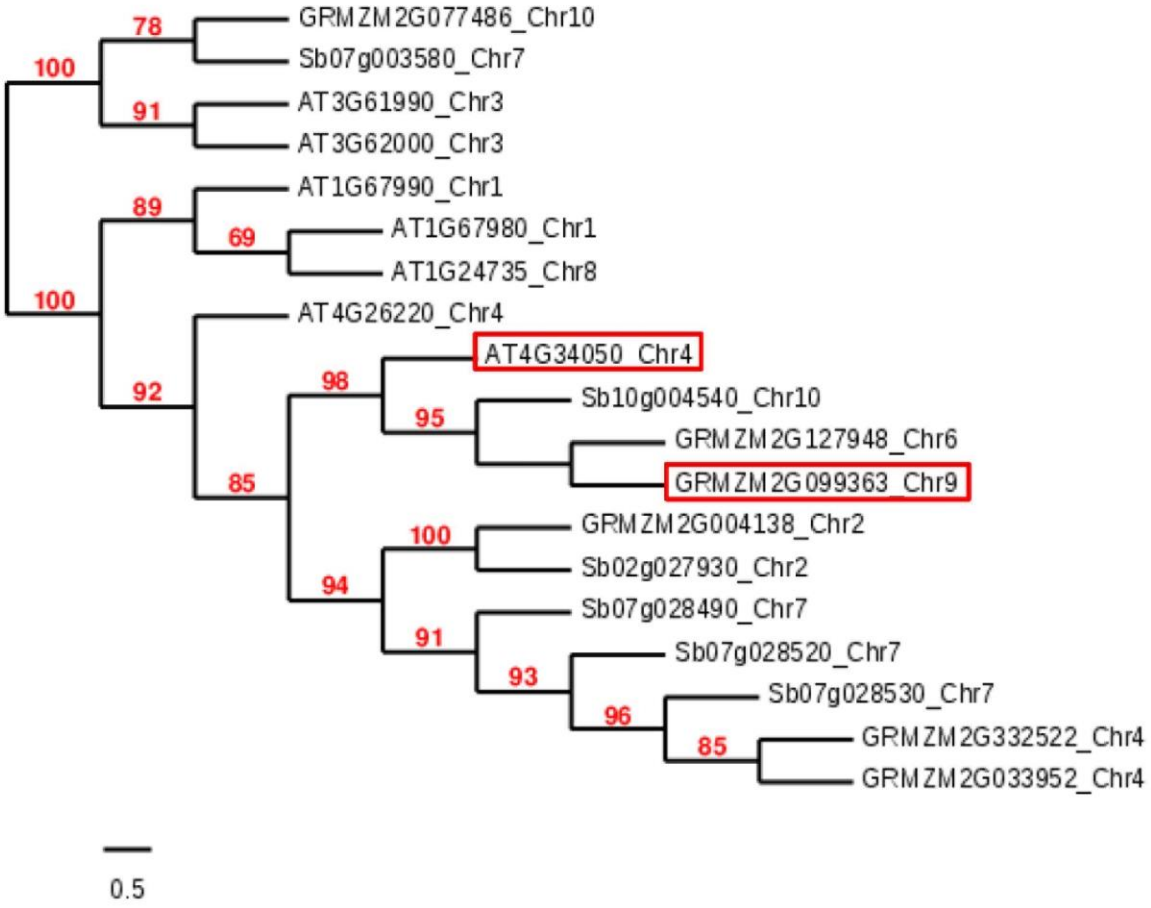

Supplementary Figure 8

Phylogenetic analysis of the CCoAOMT gene family in maize, sorghum and *Arabidopsis*, with the maximum-likelihood method implemented in the PhyML program.

The bootstrap value of each branch is indicated (100 subsamples). ZmCCoAOMT2 (corresponding to GRMZM2G099363 Chr9) and AtCCoAOMT1 (corresponding to AT4G34050 Chr4) are highlighted in red rectangle.

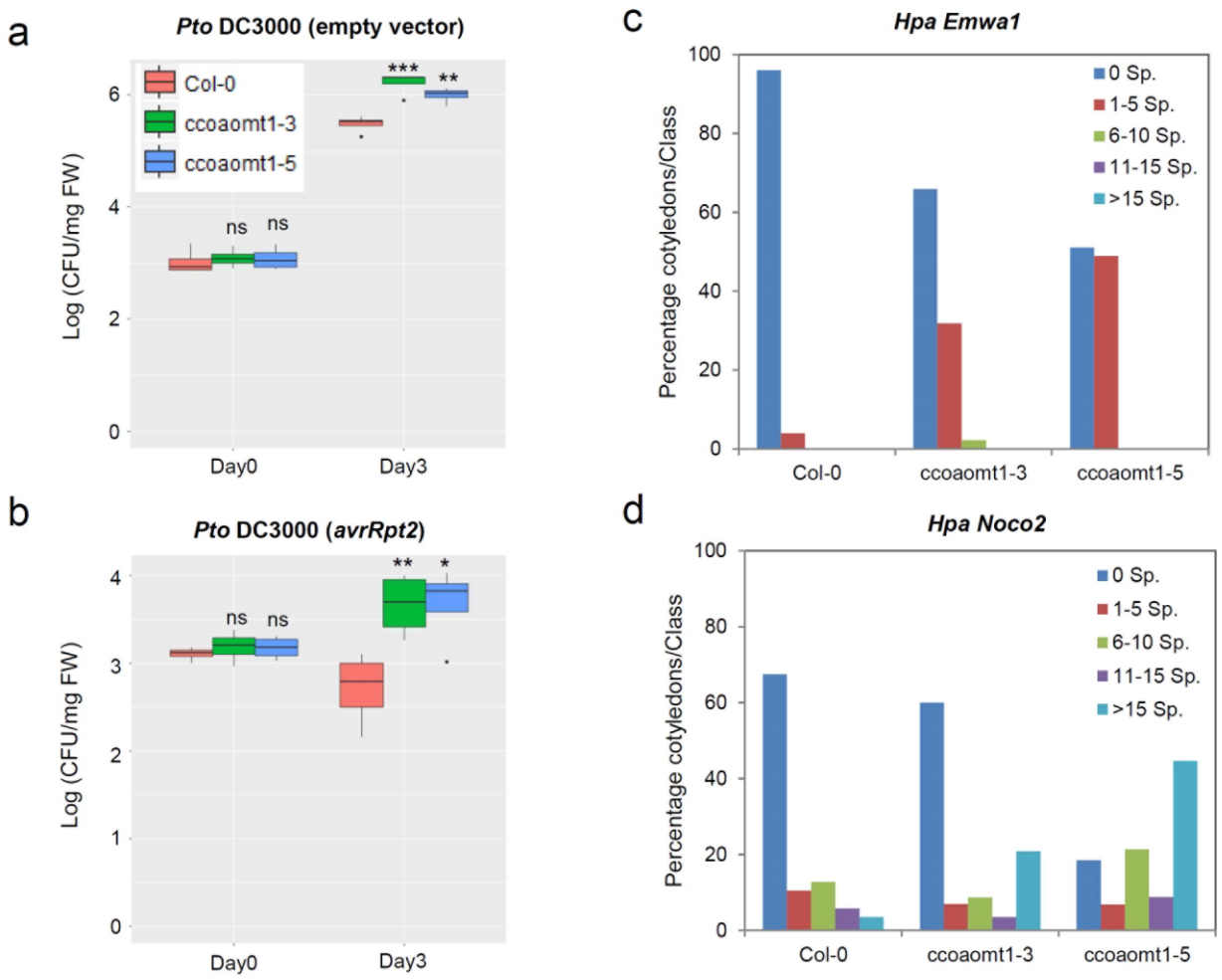

Supplementary Figure 9

Arabidopsis ccoaomt1-mutant plants showed increased susceptibility to two pathogens.

(a and b) Bacterial growth assay comparing *ccoaomt1* mutants to near-isogenic Col-0 plants. *Pseudomonas syringae* pv *tomato* (*Pto*) DC3000 (empty vector) (a) and *Pto* DC3000 (*avrRpt2*) (b) were hand-infiltrated into leaves of each genotype and counted at day 0 and day 3. $n = 3$ independent experiments. Data are $\log_{10}$-transformed colony-forming units (CFUs) per milligram. In each of the box-and-whisker plot, the center line is the median. The bottom and top edges of the boxes indicate the 25th and 75th percentiles. Whiskers mark the range of the data excluding outliers. Significant differences between mutant and Col-0 were calculated using a paired two-tailed t-test. $***P < 0.001$, $**P < 0.01$, $*P < 0.05$; ns, not significant. (c and d) *Hyaloperonospora arabidopsidis* (*Hpa)* growth assay comparing *ccoaomt1* mutants to Col-0. Sporangiophores/cotyledon were counted at 5 dpi, and cotyledons were classified. Both *ccoaomt1* mutants display more sporangiophores of *Hpa* Emwa1 (c) and Noco2 (d) than wild-type Col-0 plants. The assays were repeated twice with similar results.

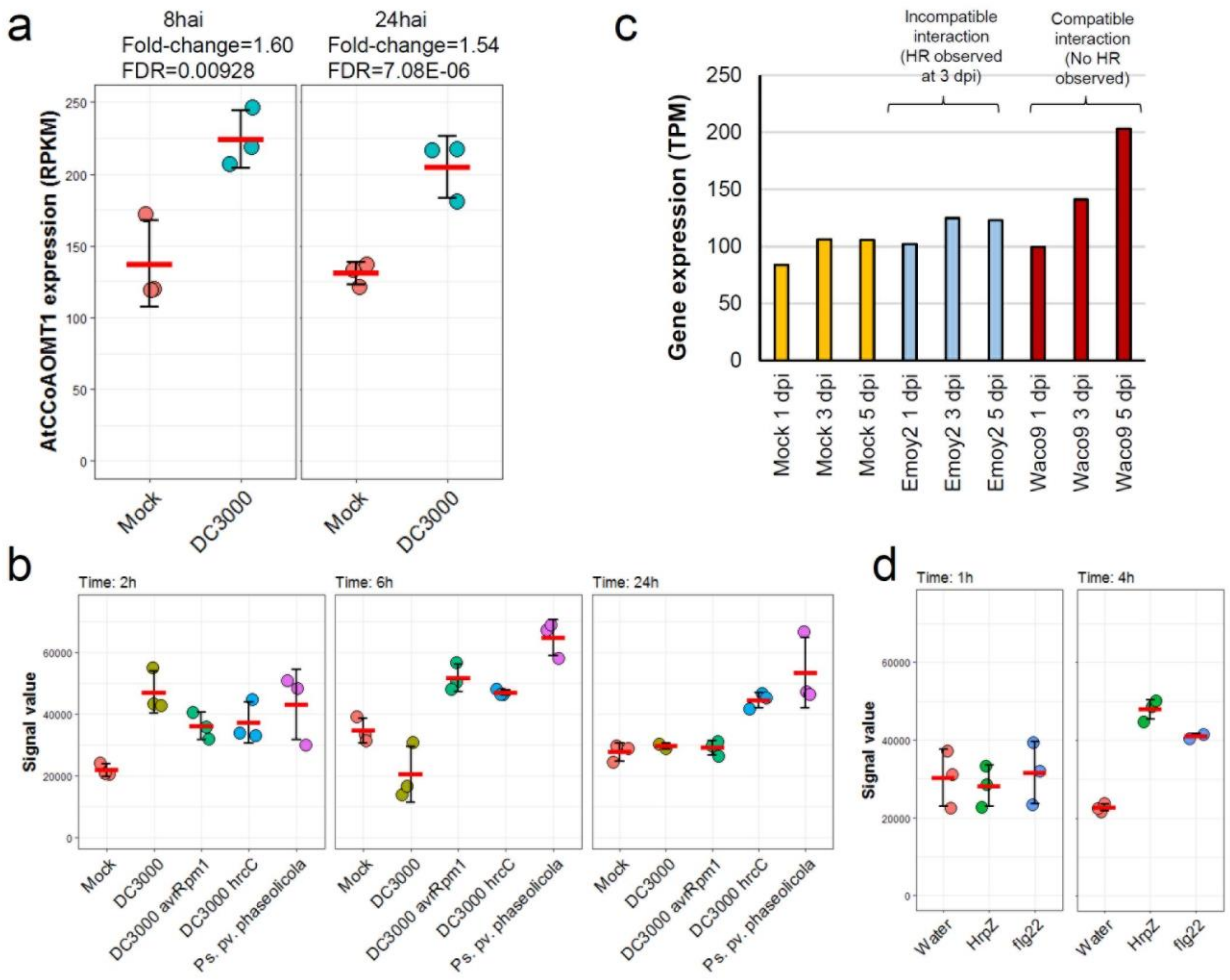

Supplementary Figure 10

AtCCoAOMT1 expression after pathogen/elicitor treatments in *Arabidopsis*.

(a) RNA-seq results derived from two-week old Col-0 seedlings sprayed with *P. syringae* DC3000 (OD=0.2) or a mock solution (10 mM $MgCl_2$, 0.04% Silwet). Gene expression is given as RPKM (Reads Per Kilobase of transcript per Million mapped reads). (b) Microarray data extracted from an additional set of experiments available at Genevestigator (from the AtGenExpress collection) also indicates that *AtCCoAOMT1* is up-regulated by bacterial infection. Pathogen inoculation was performed by hand-infiltration with a needless syringe. The figures show three independent experiments as dots, means as horizontal red lines and standard deviations as vertical black lines. (c) Time-course expression profile of *AtCCoAOMT1* upon infection with the *Hpa* isolates Emoy2 and Waco9. Data was extracted from Asai et al 2014. Gene expression is given as TPM (Tags per Million). (d) Microarray data available at Genevestigator (from the AtGenExpress collection) indicates that *AtCCoAOMT1* is up-regulated by bacterial MAMPs. The figure shows three independent experiments as dots, means as horizontal red lines and standard deviations as vertical black lines.

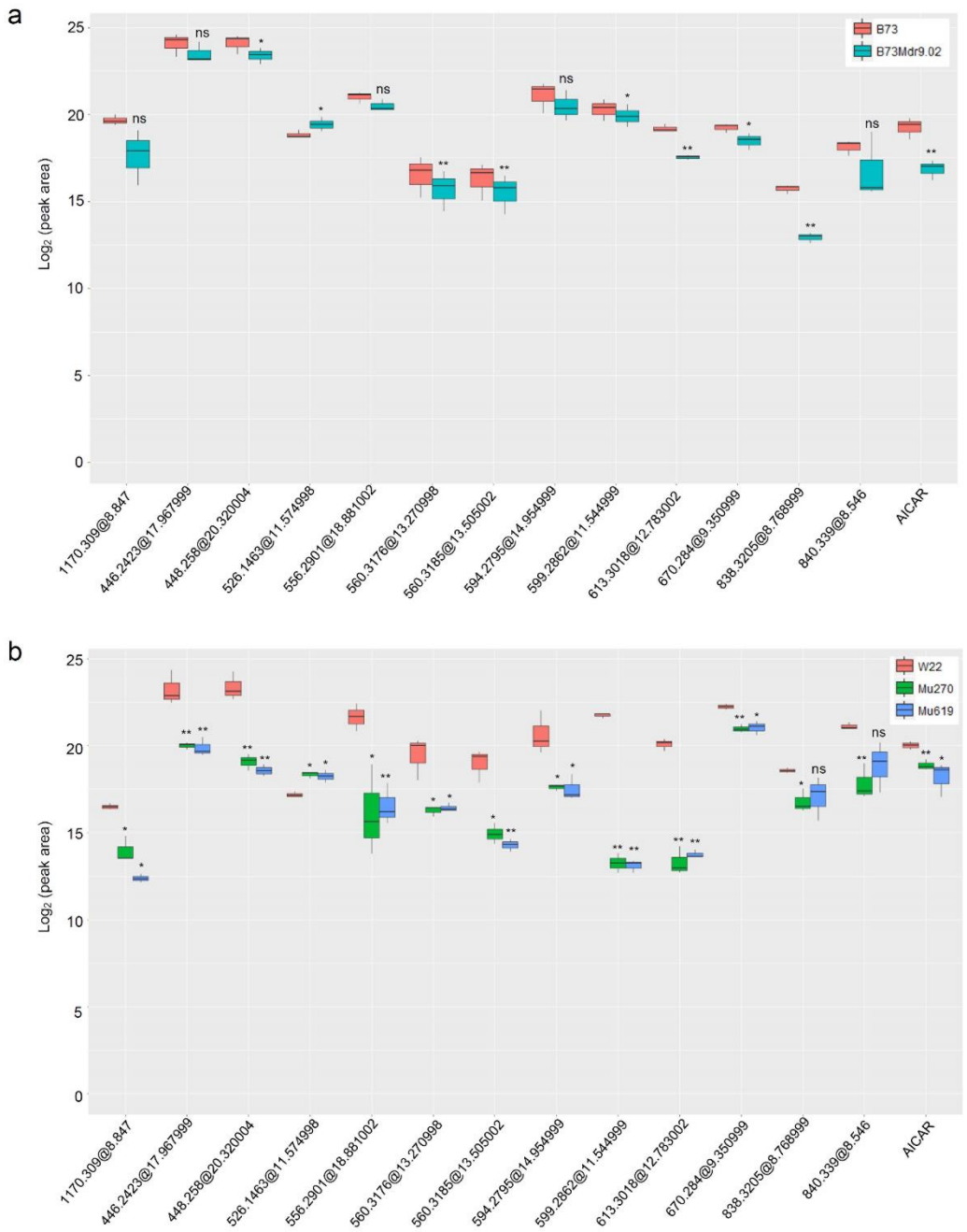

Supplementary Figure 11

Box-and-whisker plots showing relative abundance of the metabolites differentially accumulated in two sets of susceptible and resistant lines.

The ear leaf was infected with *C. heterostrophus* in the field and extracted for metabolite profiling. (a) Comparison between B73 and B73Mdr$_{9.02}$. Most chemicals showed decreased levels in the resistant line B73Mdr$_{9.02}$. (b) Comparison between the *Mu* insertion lines and W22. Similarly, resistant lines Mu270 and Mu619 have lower levels of most chemicals than susceptible line W22. Significant differences are shown at the top by a paired two-tailed t-test.

**$P < 0.01$, *$P < 0.05$; ns, not significant. Sample sizes are n=3 (3 independent experiments with each pooled 5-6 individuals per genotype) for each. In each of the box-and-whisker plot, center value is median. The bottom and top edges of the boxes indicate the 25th and 75th percentiles. Whiskers mark the range of the data excluding outliers. 'AICAR' represents '5-amino-1-(5-phospho-D-ribosyl) imidazole-4-carboxamide'. The unannotated metabolites are labeled as "accurate mass @ retention time in minute".

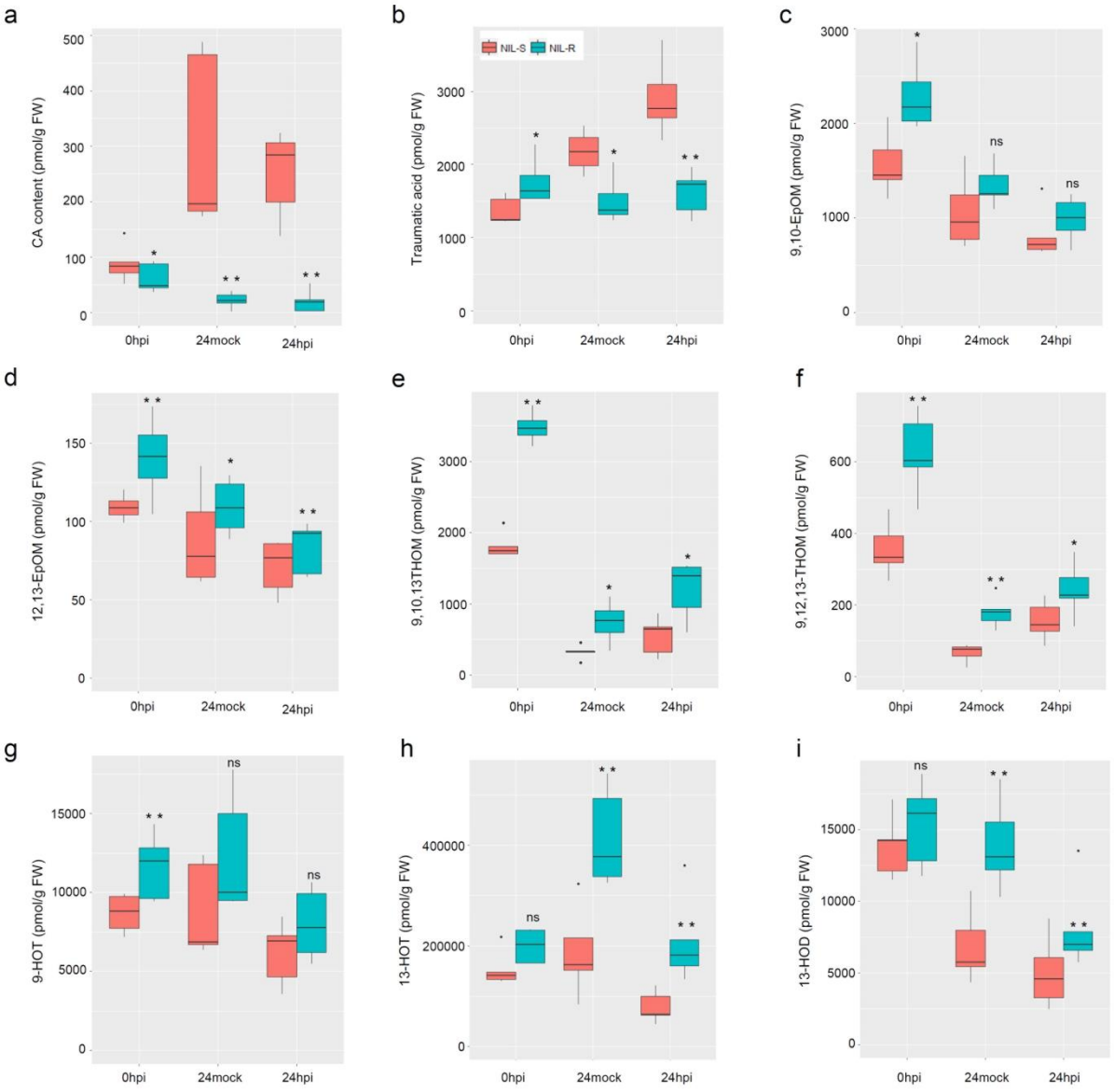

Supplementary Figure 12

Box-and-whisker plots showing levels of plant secondary metabolites produced by lipoxygenase pathways showing differential accumulation in juvenile plants of NIL-R and NIL-S infected with *C. heterostrophus*.

(a) cinnamic acid; (b) traumatic acid; (c) 9,10-epoxy octadecaenoic acid; (d) 12,13- epoxy octadecaenoic acid; (e) 9,10,13-trihydroxyoctadecaenoic acid; (f) 9,12,13-trihydroxyoctadecaenoic acid; (g) 9-hydroxyoctadecatrienoic acid; (h) 13-hydroxyoctadecadienoic acid; (i) 13-hydroxyoctadecadienoic acid. NIL-S and NIL-R differ in the ~100 kb $qMdr_{9.02}$ region with the same genetic background. 0hpi represents samples before inoculation. 24mock represents samples collected at 24 hours after inoculation with mock. 24hpi represents samples collected at 24 hours after inoculation with *C. heterostrophus*. Sample sizes are n=5 (5 independent experiments with each pooled 3 individuals per genotype) for each. Significance difference between the NILs at each treatment was indicated using a paired two-tailed t-test. $^{**}P < 0.01$, $^{*}P < 0.05$; ns, not significant. In each of the box-and-whisker plot, center value is median. The bottom and top edges of the boxes indicate the 25th and 75th percentiles. Whiskers mark the range of the data excluding outliers.

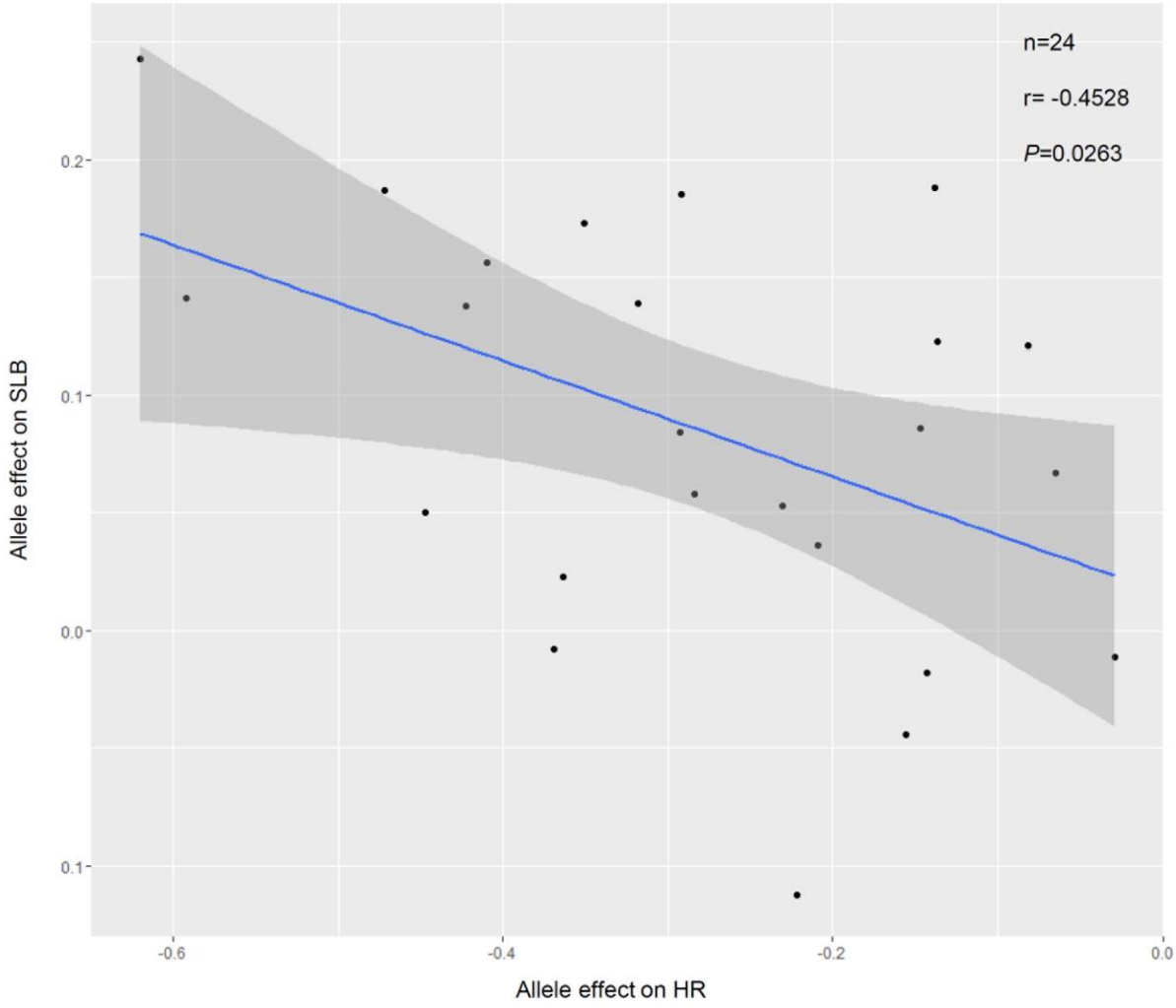

Supplementary Figure 13

Pearson's correlation coefficient between allele effects of $qMdr_{9.02}$ on SLB resistance and hypersensitive response (HR) in 24 out of 25 NAM populations.

One population generated with Hp301 and B73 was not used for HR study. Allele effects of SLB resistance is moderately negatively correlated with their effects on HR. Darker shading indicates the 95% confidence level interval. n = 24 samples. r = -0.4528 with P = 0.0263.

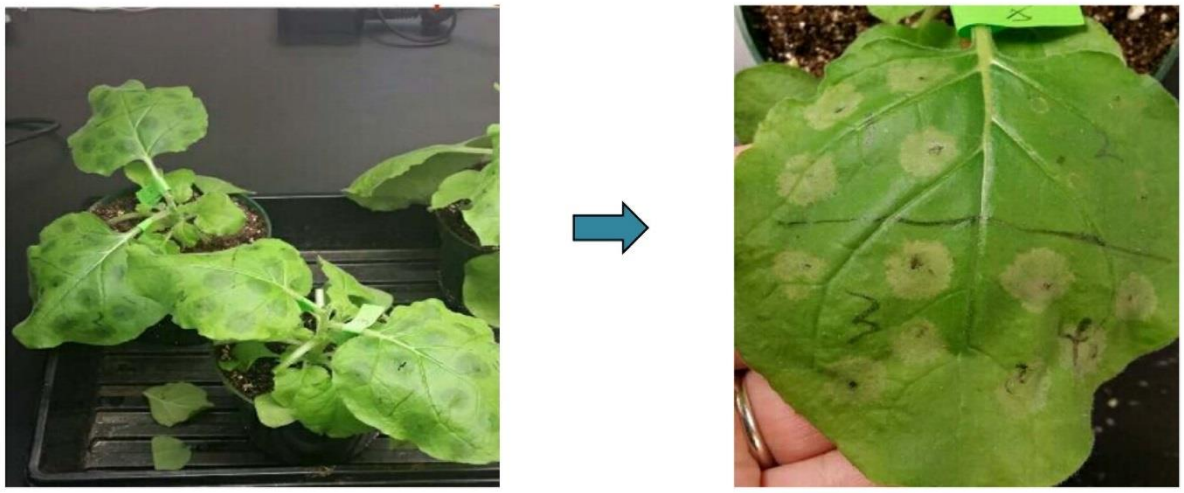

Supplementary Figure 14

Example of dynamic HR suppression assay in *N. benthamiana* leaves.

Transient co-expression was performed at several sites from multiple leaves for each gene tested. The presence of HR symptoms were recorded every day from 1-4 days after infiltration. Percentage of sites with HR was calculated at each recorded day.

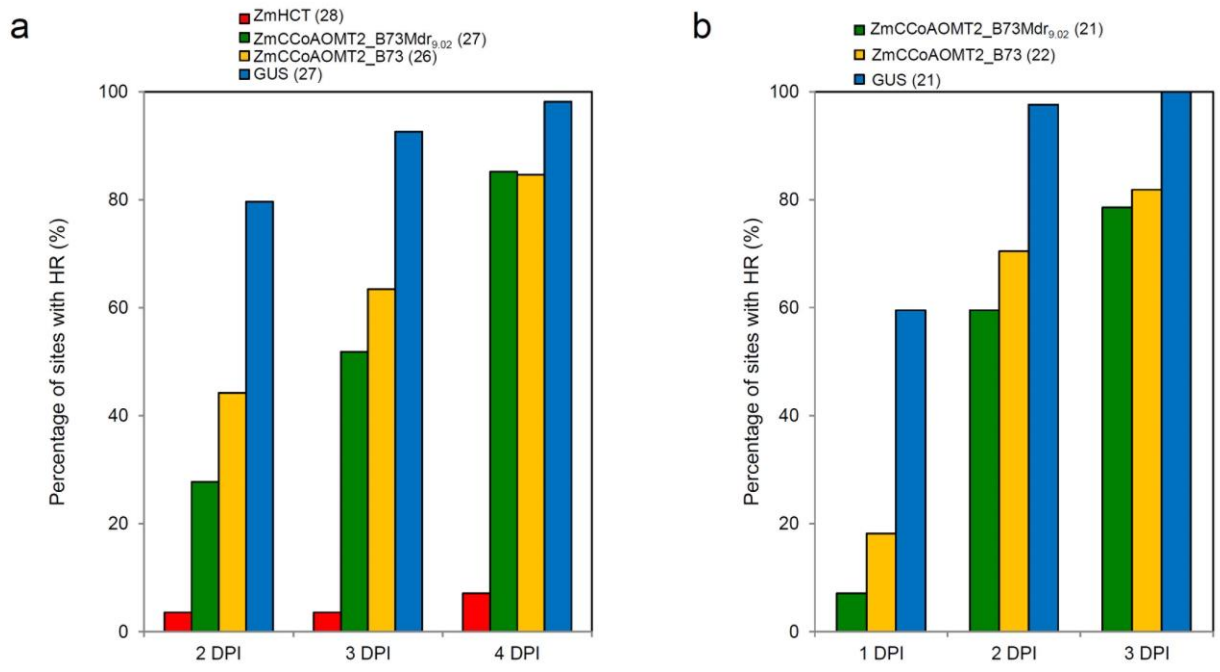

Supplementary Figure 15

Function of ZmCCoAOMT2 on suppression of HR induced by Rp1-D21 and RPM1(D505V) in *N. benthamiana* leaves.

This is the result from the second biological replicate. ZmCCoAOMT2 from B73Mdr$_{9.02}$ allele could suppress both Rp1-D21 (a) and RPM1(D505V) (b) induced HR more than B73 allele.

Supplementary Table 1. Genotype and disease scores of recombinant-derived progeny tests for SLB and GLS in the *qMdr*$_{9.02}$ region

	No. of recombinants	PZA02344	M1618	M1626	M1629	M1632	M16331	M16335	M1636	M1649	PZA03416	SLB scores		GLS scores	
												LSM±SE[3]	*P*-value[4]	LSM±SE	*P*-value
B73Mdr$_{9.02}$	na	N[1]	N	N	N	N	N	N	N	N	N	6.78±0.18	<.0001	7.05±0.10	<.0001
B73	na	B[2]	B	B	B	B	B	B	B	B	B	5.56±0.14	na	6.25±0.18	na
Type1	8	B	B	B	B	B	B	B	B	B	N	5.74±0.13	0.39	6.45±0.13	0.3879
Type2	9	B	B	B	B	B	B	B	B	N	N	5.72±0.16	0.3543	6.22±0.13	0.8752
Type3	3	B	B	B	B	B	B	B	N	N	N	5.73±0.09	0.2032	6.27±0.07	0.8842
Type4	2	N	B	B	B	B	B	B	B	B	B	5.77±0.23	0.3469	6.06±0.16	0.388
Type5	7	N	N	B	B	B	B	B	B	B	B	5.78±0.12	0.116	6.23±0.07	0.8653
Type6	3	B	B	B	N	N	N	N	N	N	N	6.95±0.05	<.0001	6.84±0.09	0.0037
Type7	3	B	B	N	N	N	N	N	N	N	N	6.75±0.14	<.0001	6.94±0.15	0.0093
Type8	3	B	N	N	N	N	N	N	N	N	N	6.68±0.09	<.0001	6.86±0.11	0.0029
Type9	4	N	N	N	N	N	N	N	B	B	B	6.91±0.07	<.0001	6.75±0.11	0.0143
Type10	2	N	N	N	N	N	N	N	N	B	B	6.84±0.08	<.0001	6.72±0.10	0.0137
Type11	8	N	N	N	N	N	N	N	N	N	B	6.74±0.09	<.0001	6.64±0.11	0.0423

Information of each molecular markers used to genotype all the plants are listed in Supplementary Table 2.
[1]N: indicates homozygous genotype identical to that of resistant parent B73Mdr$_{9.02}$;
[2]B: indicates homozygous genotype identical to B73.
[3]Data are LSmean ± SE. The disease resistance was rated using a nine-point scale with 1 being dead and 9 being the most resistant.
[4]*P*-value: Tukey's test was used to test for significant differences in resistance scores between each recombination type and B73.

Supplementary Table 2. SNP markers used in the study

SNP Name	Sequence
PZA02344	GAGAAMARTATCACTTGTTGTGGACGTTGTTGCCCGTGGCCTTGTCT[C/T]TGAGCGCGGCGCGGATCATGAACTTGAGCACGTCG AGCGGGATGTAGGTGACGATGCTGAACATCCAGATGGCGCCGCCCCACGCCCAGCCGATCCCCTGGATGCGRCAGAAGT
M1618	ACGATCGCCTTCCTTCGTCAGACCTKACAAACCAAAGCAATTAAATACGT[C/G]ATGATGAGCTACTACCAAATGACCTTCCAAGC ATAYACAGTACGTGAACTCGTATCCAGTTCCWCTGCAAACCCCC
M1626	ATCACGMCACATTTTMTGCATTCTGRAACTAGCTTTCTAGTG[T/C]ACTGTCGCAGAAGAACACTACCCACTACCCAGTGCCGCTG AAACACGATACATTCCTTGCCGATCTGGTCCACTGATCCGCCGGGAGCCGTCCCCGCCGGCC
M1629	GTCGATCATGCGACGTTGGAGAACCCGGACAGGCACCTGGACTGCATGTGTATCAGTAGGTAAATCAGGAACGAGAACATGATTA CGACCCAAAGC[C/T]AGCTTCAGCTGTGAGACGTGAAAAACCGGGTGAACTGAGCTGGAAGCAGGCAACTGAAGACGGTACGCGA CAGAGCCAATTCGCTCCAATATCTTGTATGGTCC
M1632	CGCTCGTGTCCAGGATGTACTGCGGATCATTCTTCCCCCGCGGTCAGAGACTCAGATCCCGGTCAGATTCAGCCAYTCATTGCGCY CAGCTTGTTTACCTGGTA[C/G]AGGTCGTCGCTCTTGAGCAGGCTCTTGTGGCCGACCTCGGAGTGGCGYGTCTTCTGCTCGCCGTT GCCGTTGCCGTTGGCCTGCTGCTCCTGCGCCGGTGCAG
M16331	CATATCTCCATCATGAATGGATTGTGCACTGTGATGTCGAACCAGAGAACATACTGTTAGATAAAGAATTTGAACCAAAAATTGC AGATTTTGGATTGGTTAAA[T/G]TACTAAGTCGAGGAACAGGAGCACAGATGCTGTCAAGGGTGCATGGGACTAGAGGGTACATT GCACCAGAGTGGGCTCTAAATCTTCCAATAACAGGGAAGGCT
M16335	TGGAGCAAAGACTTGAGAGTGTGCTGCCAGTGGCGCACCGGACAGTGTCC[G/A]GTGCCCTAGGCCGAGCACCACTCGAACATGC CACTCTCGGGTTTTTCCAAGCTCCGCTATAATTCATCGGACTGTCCGGTGTG
M1636	GGTTTGTACGTTGTTTATTAAAGTAGCCATTTGACTAAAACTAATTCATAG[T/C]TTTATGCATTAACTTGATTAATACCAACTCAAA TATTTCGATTCAATAATTGGTAGTGTAATCACATTATTTGTTAGCGATT
M1649	CAAATATTTAGCTTTTCAGCTAGTTTTATATAAAATAAAAGTCATCCAAAATCTGAAATATGTAATCAGTCGAGTCCTC[G/A]CGAT ATTAGAAATCCGCCAGTTTCTATATCATAAAACCTATGGATCTTTTATCTTCAGCCGCATRTAATCCCTACAATACTTARATTCTTC
PZA03416	GCAGGCACAGGTATCCACATTCCATCCTTTAATACTTCAAGCCCACCAACATCATCTTGTATCAGAAGTGTTATTGCGCCCATATCA GAATGAGATTGTAA[C/T]CCAAGAGYAAGATCAGGTTGTGGACACGGAGAATAGTAGCTAATAGTAATGTTCTGGAAAACTTCTCC AACCGCCTCTTGTATATAAGATGGTGGYAGGCT

The slash character '/' was used to mark the SNP used to genotype the mapping population. Other SNPs between B73 and B73Mdr$_{9.02}$ are indicated in different character: 'M' indicates 'A/C'; 'W' indicates 'A/T'; 'Y' indicates 'C/T'; 'K' indicates 'G/T'.

Supplementary Table 3. List of predicted genes in the *qMdr*$_{9.02}$ region

Gene ID	Chr.	Physical position (AGP_V2)		Annotated function
		Start site (bp)	End site (bp)	
GRMZM2G481291	9	16,286,452	16,295,036	F-box domain and LRR containing protein
GRMZM2G099363	9	16,320,573	16,318,197	caffeoyl-CoA O-methyltransferase
GRMZM2G099324	9	16,322,222	16,324,981	S-locus receptor like protein kinase
GRMZM2G440198	9	16,327,409	16,326,311	PIF / Ping-Pong family of plant transposases

Supplementary Table 4 Variants found in the *ZmCCoAOMT2* gene in the 26 NAM founder lines (see separate file).

Supplementary Table 5 *qMdr*$_{9.02}$ region based association analysis for SLB in maize NAM population. The r^2 value measures the linkage disequilibrium (LD) with the most significant variant with 1 being complete LD. The *P*-values is -log$_{10}$(*P*) of association with SLB resistance. (see separate file).

Supplementary Table 6. Transgenic overexpression of resistant *ZmCCoAOMT2* allele in B104 background for resistance to SLB in the field

Transgenic event	LSmean of SLB scores[2]		n[1]	*P*-value
	Non-transgenic	Transgenic positive		
B104	6.20±0.19	na	82	Na
A693B2-T_1	6.31±0.12	6.66±0.08	8/19	0.0246
A693B3-T_1	6.11±0.24	6.33±0.13	3/18	0.3774
A693B5-T_1	6.23±0.33	6.61±0.33	14/29	0.0013
A693B7-T_1	6.30±0.22	6.25±0.19	12/79	0.7051
A693B8-T_1	6.45±0.10	6.69±0.05	13/37	0.0179

[1]indicates number of plants of non-transgenic/transgenic positive plants.
[2]indicates number of plants of non-transgenic/transgenic positive plants.

Supplementary Table 7 Disease levels of four segregating *Mutator* insertion families for SLB and GLS resistance in the field.

		SLB			GLS		
		wild-type	mutant	*P*-value[3]	wild-type	mutant	*P*-value
Mu270×W22 $F_{2:3}$	n[1]	36	26	0.0273	17	10	0.0064
	LSM±SE[2]	5.11±0.04	5.35±0.04		5.59±0.11	6.01±0.09	
Mu619×W22 $F_{2:3}$	n	24	24	0.0239	15	10	<.0001
	LSM±SE	5.20±0.04	5.56±0.05		5.64±0.09	6.33±0.07	
W22×Mu270 $F_{2:3}$	n	18	17	0.0044	8	6	0.0313
	LSM±SE	4.81±0.02	5.21±0.02		5.60±0.11	5.95±0.09	
W22×Mu270 $F_{2:3}$	n	21	11	0.0447	6	4	0.0363
	LSM±SE	5.18±0.05	5.49±0.04		5.50±0.17	6.08±0.17	

[1]Number of plots for each genotype.
[2]Data are LSmean±SE. The disease resistance was rated using a nine-point scale with 1 being dead and 9 being the most resistant.
[3]Tukey's test was used to test for significant differences in resistance scores between wild-type and mutant.

Supplementary Table 8. PCR primers used in the study

Gene	Name		Primer sequence (5'-3')	Type
ZmFBXL	G1291-1	Forward	GAGATAGGGAGGAGGCGGA	cDNA amplification
		Reverse	TGTGACAGATCAGGAGACCTGC	
ZmCCoAOMT2	G9363-1	Forward	GCGACATATCAGTCGTTCGTCCA	
		Reverse	TGCTGCGCGTC GTCTACGAT	
ZmRLK	G9324-1	Forward	TGCGCTATAAGTGACCC ACC	
		Reverse	TTAAAGTTGCGCGCATGACA	
ZmCCoAOMT2	G9363-2	Forward	GCGACATATCAGTCGTTCGTCCA	NAM parental line amplification
		Reverse	TGCTGCGCGTCGTCTACGAT	
ZmFBXL	G1291-2	Forward	GGTGGCGCTGGTGAACAAGTG	qRT-PCR
		Reverse	GGCGTTGAGGTTGAGGTTGA	
ZmCCoAOMT2	RT1	Forward	GATCACCGCCAAGCACCCATG	
		Reverse	CGAGGAGCGAGTAGCCGGTGTAG	
ZmRLK	G9324-2	Forward	GTGCTTGAACGATACGGACTG	
		Reverse	CCATACTGCCTCTTGAGTTTTCA	
ZmTubulin4	Tubulin	Forward	GCTGTCCGTGGCTGAAATCACC	
		Reverse	CACCACGGTACATGAGGCAGCA	
ZmCCoAOMT2	G9363-3	Forward	gcctaggGCGACATATCAGTCGTTCGTCCA	Overexpression construct
		Reverse	cgagctcTGCTGCGCGTCGTCTACGAT	
ZmCCoAOMT2	G9363-4	Forward	GCTTGATGAGCATGTTGAGGAACTG	Transgenic line genotyping
		Reverse	CAAGGAGGCGTTTCTTTCTTTGAAT	
ZmCCoAOMT2	G9363-5	Forward	CGCGCAGCATTAAACTATCA	*Mutator* insertion line genotyping
		Reverse	ACCGGTTCGATAGTGAGACG	
	MuTIR6		AGAGAAGCCAACGCCAWCGCCTCYATTTCC	
ZmCCoAOMT2	G9363-$Mdr_{9.02}$	Forward	GGGGACAAGTTTGTACAAAAAAGCA	Construct for HR test
			GGCTCCATGGCCACCACGGCGACC	
		Reverse	GGGGACCACTTTGTACAAGAAAGCTGGGT	
			GCTTGACGCGGCGGCAGAG	
ZmCCoAOMT2	G9363-B73	Forward	GGGGACAAGTTTGTACAAAAAAGCAGGCT	
			CCATGGCCACCACGGCGACCG	
		Reverse	GGGGACCACTTTGTACAAGAAAGCTGGGT	
			GCTTGACGCGGCGGCAGAGCG	
At4G34050	At4050	Forward	GGCAGCAAACAGTTACTACAG	Arabidopsis mutant genotyping
		Reverse	CCTGAGTTCCTTCATTGATTC	
	DHSAL		CCACCATCAAACAGGATTTTCGCCTGCTGGG	